frontiers in Earth Science

ORIGINAL RESEARCH
published: 27 July 2021
doi: 10.3389/feart.2021.697170

Architectural Diversity of Submarine Lobate Deposits

Tim R. McHargue[1]*, *David M. Hodgson*[2] *and Eitan Shelef*[3]

[1]Department of Geological Sciences, School of Earth, Energy and Environmental Sciences, Stanford University, Stanford, CA, United States, [2]Stratigraphy Group, School of Earth and Environment, University of Leeds, Leeds, United Kingdom, [3]Department of Environmental Sciences, University of Pittsburgh, Pittsburgh, PA, United States

Lobate deposits in deep-water settings are diverse in their depositional architecture but this diversity is under-represented in the literature. Diverse architectures result from multiple factors including source material, basin margin physiography, transport pathway, and depositional setting. In this contribution, we emphasize the impact of differing source materials related to differing delivery mechanisms and their influence on architecture, which is an important consideration in source-to-sink studies. Three well imaged subsurface lobate deposits are described that display three markedly different morphologies. All three lobate examples, two from intraslope settings offshore Nigeria and one from a basin-floor setting offshore Indonesia, are buried by less than 150 m of muddy sediment and are imaged with high resolution 3D reflection seismic data of similar quality and resolution. Distinctively different distributary channel patterns are present in two of the examples, and no comparable distributaries are imaged in a third example. Distributary channels are emphasized because they are objectively recognized and because they often represent elements of elevated fluid content within buried lobate deposits and thus influence permeability structure. We speculate that the different distributary channel patterns documented here resulted from different processes linked to source materials: 1) a lobate deposit that is pervasively channelized by many distributaries that have branched at numerous points is interpreted to result from comparatively mud-rich, stratified, turbulent flows; 2) an absence of distributaries in a lobate deposit is interpreted to result from collapse of mud-poor, turbulent flows remobilized from littoral drift; and 3) a lobate deposit with only a few, long, straight distributaries with few branching points is interpreted to be dominated by highly viscous flows (i.e., debris flows). We propose a conceptual model that illustrates the relationship between the proportion of mud in contributing flows and the relative size and runout distance of lobate deposits. We conclude that reconciling 3D seismic morphologies with outcrop observations of channels, scours, and amalgamation zones, and simple application of hierarchical schemes, is problematic. Furthermore, when characterizing unconfined deep-water deposits in the subsurface, multiple models with significant differences in predicted permeability structure should be considered.

Keywords: submarine fan, submarine lobe, submarine channel, turbidite, debris flow, distributary, seismic geomorphology

OPEN ACCESS

Edited by:
Rosanna Maniscalco, University of Catania, Italy

Reviewed by:
Roberto Tinterri, University of Parma, Italy
Yvonne Therese Spychala, Leibniz University Hannover, Germany

***Correspondence:**
Tim R. McHargue
timmchar@stanford.edu

Specialty section:
This article was submitted to Sedimentology, Stratigraphy and Diagenesis, a section of the journal Frontiers in Earth Science

Received: *19 April 2021*
Accepted: *12 July 2021*
Published: *27 July 2021*

Citation:
McHargue TR, Hodgson DM and Shelef E (2021) Architectural Diversity of Submarine Lobate Deposits. Front. Earth Sci. 9:697170. doi: 10.3389/feart.2021.697170

INTRODUCTION

Submarine fans and other submarine lobate deposits are repositories of continentally-derived coarse sediment in the deep sea (e.g., Normark, 1978), and are important archives of palaeoenvironmental change. The potentially large volumes of sand in lobate deposits make them important targets for hydrocarbon exploration and production (Weimer et al., 2000) as well as potentially important aquifers, or reservoirs for the sequestration of CO_2 or hazardous fluids (Ketzer et al., 2005). Simulations of fluid dynamics within lobate deposits designed to optimize performance, either during fluid injection or extraction, necessitate a detailed understanding of depositional architecture, heterogeneity distribution, and permeability structure.

Diverse conceptual models of submarine fan deposits have been proposed (e.g., Normark, 1970; Mutti and Ricci Lucchi, 1972; Walker, 1978; Stow, 1985; Stow, 1986; Reading and Richards, 1994). Tectonic setting, source terrain, sediment transport mechanisms, and bathymetric irregularities have long been acknowledged to be important when predicting the characteristics of submarine fans (Normark, 1970; Mutti and Ricci Lucchi, 1972; Stow, 1985; Stow, 1986; Reading and Richards, 1994). Early submarine fan models included a diverging set of channel-levee complexes each of which terminated at the distal end with a sand-rich "depositional lobe" (Normark, 1970; Mutti and Ghibaudo, 1972). More recent studies with more complete or detailed data demonstrate that lobate deposits at the terminus of each distributary channel complex typically consist of multiple smaller, nested or overlapping offset lobate to palmate bodies (e.g., Mutti, 1977; O'Connell et al., 1991; Lowry et al., 1993; Martinsen et al., 2000; Sullivan et al., 2000; Johnson et al., 2001; Gardner et al., 2003; Posamentier and Kolla, 2003; Hodgson et al., 2006; Deptuck et al., 2008; Prélat et al., 2009; Groenenberg et al., 2010; Mulder and Etienne, 2010; Prélat and Hodgson, 2013; Picot et al., 2016).

The presence of channels in at least some lobate deposits has long been recognized (Beaubouef et al., 1999; Carr and Gardner, 2000; Sullivan et al., 2000; Gardner et al., 2003). Normark (1970), in his classical and commonly cited model, included shallow distributary channels in the proximal portion of his definition of a lobe but few to none in the distal portion of the lobe. This model has been widely adopted and applied by many subsequent researchers (summarized in Mulder and Etienne, 2010). A distinct levee-confined distributary channel network is present in the proximal lobe, costructed as the upper mud-rich portion of mud-rich stratified flows overspills channel confinement. Resistance to shear of the mud-rich levees sustains confinement although levee height, shear resistance and channel depth decrease down flow. Farther down flow, as the turbulent flow becomes increasingly sand-rich, the basal part of the flow collapses at the distributary channel mouth and produces a tabular sand deposit.

More recent fan models (Prélat et al., 2009; Mulder and Etienne, 2010; Prélat et al., 2010) highlight the scaling of lobes, but do not emphasize distributary channels within depositional lobes. This is important because the potential presence and distribution of channels within lobate deposits can strongly affect the permeability structure of the deposit. Relative to the non-channelized portion of a lobate deposit, sand caliber can be coarser, and thus permeability higher within channels so that channel deposits may be a preferred pathway for subsurface fluids (Pyles et al., 2014; Jones et al., 2015; Hofstra et al., 2017; Bell et al., 2018). In contrast, models of intraslope lobe complexes (Spychala et al., 2015; Jobe et al., 2017) or transient fans (Adeogba et al., 2005) above stepped submarine slope profiles, emphasise channels that cut through lobes after accommodation is healed.

In modern or near modern turbidite systems, distributary channels have been imaged within lobate deposits in some cases (O'Connell et al., 1991; Twichell et al., 1992; Kidd, 1999; Posamentier and Kolla, 2003; Hadler-Jacobson et al., 2005; Clark and McHargue, 2007; Hadler-Jacobson et al., 2007; Bourget et al., 2010; Bakke et al., 2013; Doughty-Jones et al., 2017; Howlett et al., 2020). However, even in modern submarine fan systems, detailed bathymetric records and sidescan sonar recordings often do not produce clear images of distributary channel networks within lobate deposits (Bonnel et al., 2005; Gervais et al., 2006; Jegou et al., 2008; Dennielou et al., 2009; Bourget et al., 2010; Hanquiez et al., 2010; Migeon et al., 2010) even though incisional transient fan channels, when present, may be well imaged (Johann et al., 2001; Adeogba et al., 2005; Gamberi and Rovere, 2011; Maier et al., 2011; Barton, 2012; Maier et al., 2012; Prather et al., 2012a; Maier et al., 2013; Yang and Kim, 2014).

Outcrop studies of lobate deposits with laterally extensive exposures have guided fundamental concepts of fan architecture and facies distribution (Mutti and Ricci Lucchi, 1972; Martinsen et al., 2000; Sullivan et al., 2000; Johnson et al., 2001; Gardner et al., 2003; Hodgson et al., 2006; Prélat et al., 2009; Groenenberg et al., 2010; Prélat and Hodgson, 2013). However, there are few opportunities to unambiguously document the three-dimensional relationships of architectural components within lobate deposits in outcrop exposures. Interestingly, these few examples display conspicuous differences. The somewhat lobate deposits of the Brushy Canyon Formation in Texas, United States, are extensively channelized with tabular sands in overbank positions (e.g., Gardner et al., 2003). The Ross Formation, Ireland, displays well developed tabular sandstone units associated with multiple channels (e.g., Martinsen et al., 2000; Sullivan et al., 2000; Pyles and Jennette, 2009; Pierce et al., 2018). In the Skoorsteenberg Formation in the Tanqua Karoo Basin, South Africa, the lobate deposits with the most continuous and extensive exposure (e.g., Johnson et al., 2001; Hodgson et al., 2006; Prélat et al., 2009; Groenenberg et al., 2010; Prélat and Hodgson, 2013), conventional channels, such as seen in the Ross Formation, are present only in the most proximal exposure of the lobate units (Johnson et al., 2001; Hodgetts et al., 2004; Hodgson et al., 2006; Hofstra et al., 2017). Distally, zones of amalgamation have been interpreted as possible channels within lobate depositional units (Johnson et al., 2001; Hodgetts et al., 2004). However, these outcrop examples lack constraints on source material, basin margin

TABLE 1 | Tabular summary of contextual data and observations associated with each of the three discussed lobate examples.

	Lobate examples		
	1	2	3
Water depth	2,250 m	1,275 m	2,000 m
Burial thickness	120 m	50 m	160 m
Seismic dominant frequency	60 Hz	60 Hz	50 Hz
Seismic resolution	8.3 m	8.3 m	10 m
Sediment source	Major delta	Major delta	Major delta
Sediment delivery	Large leveed channel complex	From littoral drift via multiple small non-leveed gullies	Large erosional channel complex
Depositional setting	Mid slope	Mid slope	Base of slope
Length (L)	12 km	14 km	7 km
Width (W)	14 km	6 km	7 km
Maximum thickness (T)	130 m	20 m	43 m
Aspect ratio (W/T)	108	300	163
Branching nodes	Pervasive	0	1
Distributary number	Pervasive	0	Few (~5)
Surface texture	Channelized	Smooth with scours	Nodular to smooth
Dominant process	Turbulent stratified flows with thick dilute layer	Collapse of turbulent stratified flows with thin dilute layer	Debris flows abundant to dominant

physiography, or transport pathways, and their control on depositional architecture, which limit their utility within source-to-sink contexts.

In deep subsurface examples, images of submarine lobate deposits, even in high quality 3D reflection seismic volumes, often reveal few, if any, details of architectural features within or on the surface of lobate deposits. In some cases, lens-shaped lobate deposits, typically stacked in a compensating pattern (*sensu* Mutti and Sonnino, 1981), can be recognized within a larger lobate system (e.g., Gervais et al., 2006; Deptuck et al., 2008; Saller et al., 2008; Bourget et al., 2010; Prélat et al., 2010; Yang and Kim, 2014), but even these gross features may not be resolved in the deep subsurface. Consequently, more often than not, the presence of distributary channels and other architectural features of lobate deposits are inferred based on models, about which there is considerable uncertainty.

We recognize that the range of architectures within lobate deposits is diverse and that this diversity is under-represented in the literature. Therefore, the objective of this paper is to emphasize this diversity by describing three examples of lobate deposits with fundamentally different architectures. We describe the context within which each lobate deposit is found and suggest possible controlling mechanisms. The sinuosity, distribution, and divergence of channels, if present, are key criteria for discriminating between these three examples. These examples were chosen because of their distinctly different architectures as imaged in 3D reflection seismic data with very similar resolution (**Table 1**). All three are likely late Pleistocene in age, buried by about 50–160 m of muddy sediment. All three are similar in size and located on passive margins offshore of large deltas, which are the source of their sediment. Two are located in intraslope basins offshore of the Niger Delta, Nigeria, while the third is located on the basin floor offshore of the Mahakam Delta, Kalimantan, Indonesia (**Figure 1**). No cores are available to confirm interpretations of sediment caliber and distribution. However, seismic Root Mean Squared (RMS) amplitude displays provide an objective basis for a general interpretation of mud versus sand (Posamentier and Kolla, 2003).

DESCRIPTION OF THREE EXAMPLES

In the description of the three examples below we use the general term "lobate deposit" because hierarchical classification originally designed for two-dimensional reflection seismic and outcrop data (e.g., Deptuck et al., 2008; Prélat et al., 2009; Mulder and Etienne, 2010; Prélat and Hodgson, 2013) does not apply directly to deposits imaged by three-dimensional reflection seismic data. We revisit this topic in the discussion.

Lobate Example 1: A Pervasively Channelized Lobate Deposit

Example 1: Regional Setting

Lobate Example 1 (LE1) is located on the continental slope of the western Niger Delta approximately 95 km from the modern shelf edge beneath 2,250 m of water (**Figure 1A**). The general direction of sediment transport was from north to south or southwest. The continental slope in the study area is irregular (i.e., the stepped profile of Prather et al., 1998; Prather, 2003), including areas of both high and low gradient, as well as ridges that are elevated above the regional slope profile (Allen, 1965; Doust and Omatsola, 1990; Damuth, 1994; Pirmez et al., 2000; Steffens et al., 2003). The steep segments of the profile are formed on the seaward flanks of basinward verging thrusts cored by over-pressured buoyant mud. The areas of low gradient (i.e., steps of Prather et al., 1998) occur on the landward sides of the thrust ridges. LE1 accumulated within a sediment wedge on one of these steps in what has been called a slope apron (Gorseline and Emery, 1959; Barton, 2012; Prather et al., 2012a) within healed slope accommodation (Prather, 2000; Prather, 2003; Barton, 2012; Prather et al., 2012a; Sylvester et al., 2012).

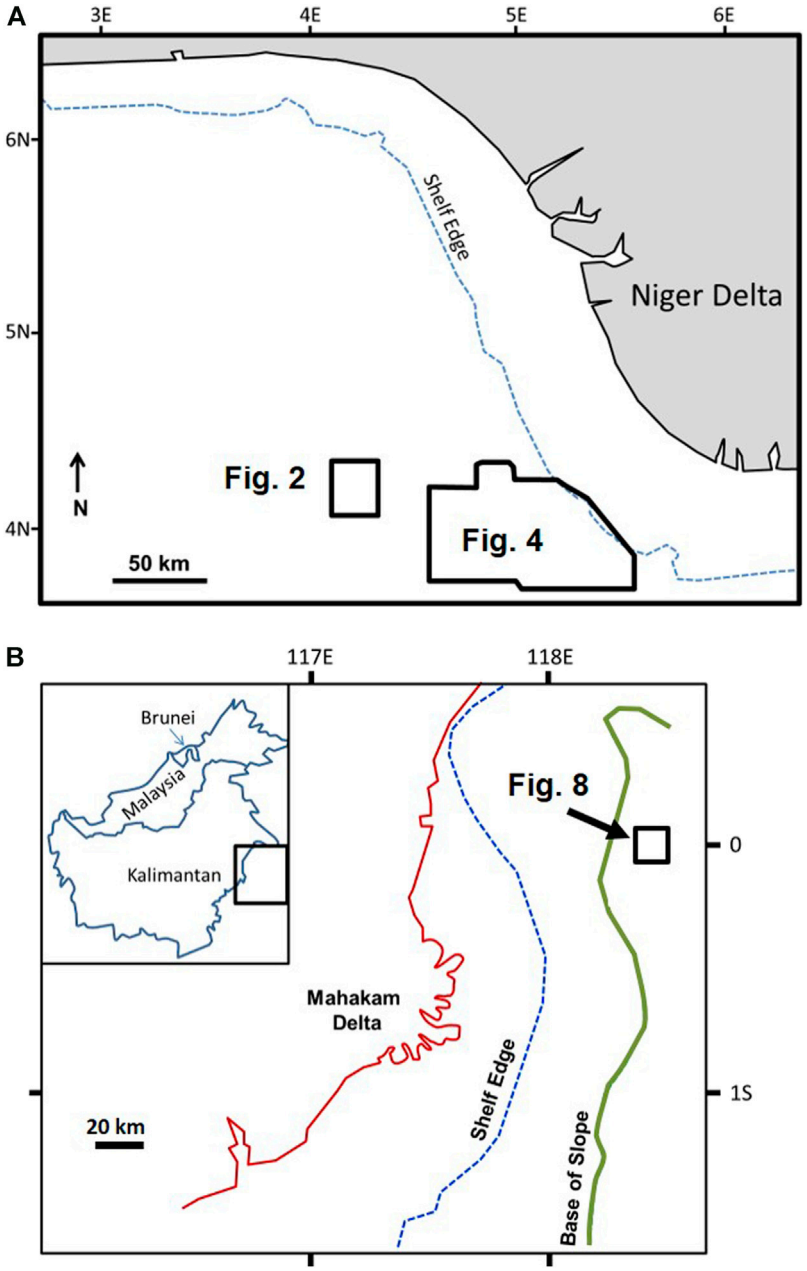

FIGURE 1 | (A) map of a portion of offshore Nigeria. The location of panels 2, 4 are indicated. **(B)** map of a portion of offshore Kalimantan, Indonesia. The location of panel 8 is indicated.

Example 1: Seismic Data

Images of LE1 (**Figures 2**, **3**) are derived entirely from industry standard 3D reflection seismic data. The interpreted data have a dominant frequency of about 60 Hz at the shallow depth of the studied lobate deposit, which assuming an acoustic velocity of 2,000 m/sec (Flood et al., 1997), provides a nominal vertical resolution of approximately 8.3 m (**Table 1**). Sample spacing is 4 milliseconds (ms) and bin spacing is 12.5 m by 12.5 m. Planform images are horizon-referenced displays garnered from the uppermost 200 ms (200 m) of data below the seabed. The contiguous seismic volumes that encompass LE1 cover an irregularly shaped area of approximately 5,500 km^2, of which, about 500 km^2 are displayed in **Figures 2**, **3**. The seismic volumes extend from near the modern shelf edge to a position on the continental slope approximately 110 km seaward from the shelf edge.

Example 1: Description

LE1 (**Figures 2**, **3**) has been described previously and called a lobe complex (Prélat et al., 2010, their Figure 5). These authors noted that LE1 is the youngest of several related lobate units. Each

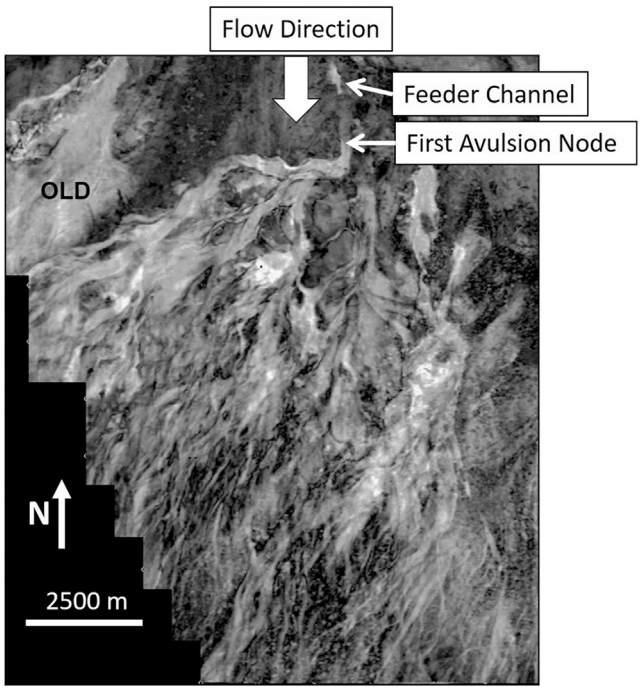

FIGURE 2 | An RMS (Root Mean Squared) amplitude extraction of LE1 from a 3D reflection seismic volume on the middle slope, offshore Nigeria (see **Figure 1** for location). Sediment transport is from north to south. The image is calculated from the interval between 10 and 20 ms from the top of the lobate deposit (see **Figure 3**). High RMS values are displayed as white to yellow colors. An older lobate deposit (marked OLD) is present to the west of LE1. Modified from Prélat et al. (2010).

lobate unit is displaced eastward of its predecessor, occupying low topography between the mounded sediment of the previous lobate deposit to the west and the regional southwest-dipping slope to the east (Prélat et al., 2010).

LE1 is approximately 14 km wide, in excess of 12 km long, with a maximum thickness of 130 m near the proximal (North) end of the lobe, yielding a width to thickness ratio of 108 (Prélat et al., 2010). LE1 is buried by approximately 120–170 m of mud-rich sediments. No core samples are available from LE1.

The single feeder channel complex (approximately 600–700 m wide) to LE1 was confined by a combination of erosion and outer, or external, levee aggradation (**Figures 3A,B**). Outer levees flanking the feeder channel complex are up to 50 m thick and 500 m wide, represented in reflection seismic data by low Root Mean Squared (RMS) amplitude values (**Figures 3A,B**). Sediment from the single levee-confined feeder channel complex was dispersed across LE1 via a system of distributary channels, each 300 m or less in width (**Figures 2**, **Figures 3A**). Numerous branching points resulting either from avulsion or bifurcation, are observed within the distributary channel system all across LE1 (**Figure 2**). For approximately 3 km down flow from the first, most proximal, branching point, distributary channels continue to be flanked by small outer levees, although levee height decreases down flow to the south until they are no longer resolvable on seismic profiles (**Figure 3C**). Fill within these proximal distributary channels, as well as within the feeder channel complex, are recorded as high RMS values (**Figure 3**).

In a down-flow (southward) direction, each levee-confined distributary channel transitions into numerous sub-parallel to slightly diverging smaller channels (100 m or less in width) that form a 2–3 km wide cluster (**Figure 2**). The channel pattern in each cluster is achieved by increasing the number and frequency of branching points distally so that a few channels in a proximal position increase distally to a large number of closely spaced channels toward the fringe of LE1. Despite the fact that limited vertical resolution results in compositing multiple vertically juxtaposed channels within the same image, the entire lobate unit beyond the limit of levee confinement appears to consist of numerous channel clusters. The axis of each cluster follows a path that is sub-parallel to the axis of adjacent clusters and thus the overlap between adjacent clusters is minimal.

Within LE1, depositional lenses have been interpreted (Prélat et al., 2010) as lobes and can be resolved in at least some seismic profiles in the proximal to middle, high relief portion of LE1 (**Figures 3C,D**). Distally, the lenses gradually become flatter and thinner until they are no longer distinguishable (**Figure 3E**).

Lobate Example 2: A Lobate Deposit Without Distributary Channels

Example 2 Regional Setting

LE2 is located on the continental slope of the Niger Delta (**Figures 1**, **4–7**), 70 km southeast of LE1 and approximately 45 km basinward of the modern shelf edge beneath 1,275 m of water (**Figure 1A**). The general direction of sediment transport was from northeast to southwest. As is the case with LE1, LE2 is in an area of relatively low gradient along an irregular stepped profile resulting from deep seated thrusts modified by diapiric deformation of buoyant shales (circular features near the head of LE2 in **Figure 6**) (Allen, 1965; Doust and Omatsola, 1990; Damuth, 1994; Pirmez et al., 2000; Steffens et al., 2003). LE2 accumulated as part of a slope apron (Gorseline and Emery, 1959; Barton, 2012; Prather et al., 2012a) within healed slope accommodation (Prather, 2000; Prather, 2003; Barton, 2012; Prather et al., 2012a; Sylvester et al., 2012).

Example 2 Seismic Data

Images of LE2 are derived entirely from industry standard 3D reflection seismic data of very similar vintage and quality to the data that are illustrated for LE1 (**Table 1**). About 6,000 km^2 of contiguous 3D reflection seismic data have been examined in the area around LE2 (**Figure 4**) including the shelf edge near LE2 as well as surrounding slope features. As with LE1, these interpreted data have a dominant frequency of about 60 Hz at the shallow depth of the studied lobate deposit, which assuming an acoustic velocity of 2,000 m/sec (Flood et al., 1997), provides a nominal vertical resolution of approximately 8.3 m (**Table 1**). Sample spacing is 4 milliseconds and bin spacing is 12.5 m by 12.5 m. The plan view images provided in this paper for LE2 are horizon-referenced displays of data between 50 and 150 milliseconds (50–150 m) below the seabed.

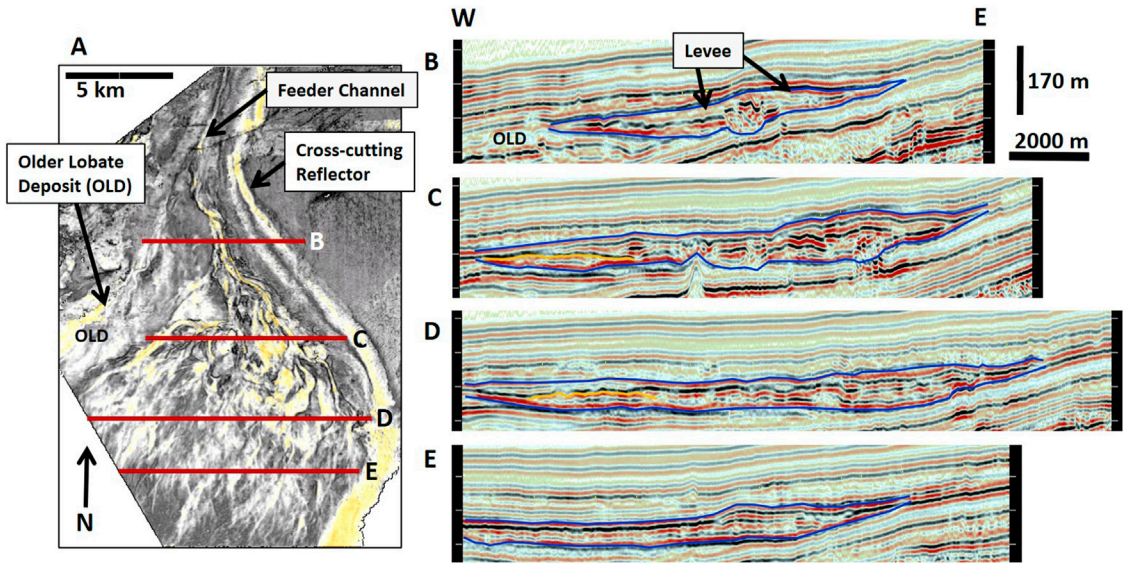

FIGURE 3 | Cross sections through LE1 from a 3D reflection seismic volume. **(A)** Plan view Root Mean Squared (RMS) amplitude extraction midway between the upper and lower bounding surfaces of LE1 [blue horizons in panels **(B–E)**] superimposed on a continuity display (lateral rate of change of RMS amplitude values from the same interval). High RMS values are displayed as white to yellow colors. Low continuity values are displayed as black. Modified from Prélat et al. (2010). The locations of cross-sections **(B–E)** are displayed as red lines. An older lobate deposit (OLD) is present to the west and beneath LE1. **(B)** Proximal section through the feeder channel complex for LE1. Prominent levees are present on both sides of the channel complex and thin away from the channel complex. **(C)** Seismic section through the proximal portion of LE1. This portion of the lobate deposit is characterized by highly discontinuous reflections resulting from the presence of numerous distributary channels. As an example, the top of a single lens-shaped unit within LE1 is highlighted as a yellow horizon. **(D)** Seismic section through the medial portion of LE1. This portion of the lobate deposit is characterized by moderately discontinuous reflections, resulting from the presence of numerous distributary channels. The top of one lens-shaped unit within LE1 is highlighted as a yellow horizon. **(E)** Seismic section through the distal portion of LE1. This portion of the lobate deposit is characterized by moderately continuous reflections. Very small distributary channels appear to be present in plan view but are too small (shallow) to break up reflection continuity in section view. Lens-shaped units within LE1 are not resolvable.

Example 2 Description

LE2 is approximately 6 km wide, 14 km long, and a maximum of 20 m thick yielding a width to thickness ratio of 300 (**Table 1**). LE2 is buried at approximately 50 m below the seabed. No core samples are available from LE2.

In cross-section, LE2 is tabular and thin (**Figure 7**) and distinct internal lens shapes, if present, are not resolved with available data. LE2 is a high amplitude feature (HAF) displayed in the RMS extractions of **Figure 4** through **Figure 7** as a light colored object (elevated RMS values). Several HAFs of diverse sizes and shapes are displayed on the continental slope surrounding LE2 including narrow linear HAFs, fan-shaped HAFs, and irregular broad HAFs that indicate the location and transport path of granular clastic material.

In the area north and east of LE2, the shelf edge has a generally smooth to slightly irregular northwest trend (**Figure 4**). No submarine canyon is imaged at or near the shelf edge. Instead, the shelf edge occasionally is offset landward by approximately 2 km by arcuate indentations that are 5–8 km wide (**Figure 4**). Numerous narrow and linear HAFs (interpreted as gullies) are imaged immediately basinward of the arcuate indentations (area X in **Figure 4**). Some of the linear HAFs appear to terminate down slope, after 5–10 km or less, in small divergent, fan shaped HAFs that are only one or 2 km wide and long (area X, **Figure 4**). Others continue farther down slope and are focused by bathymetry into larger HAFs with stronger amplitudes.

Directly up slope from LE2, the shelf edge is beyond the limit of the seismic volume (**Figures 4**, **5**). In the most proximal portion of the seismic volume, numerous narrow linear HAFs each give way down slope to a wedge-shaped HAF consisting of a divergent collection of sharp to diffuse linear forms with elevated amplitude (area Y, **Figures 4**, **5**). The wedge-shaped HAFs overlap to form an apron (sensu Reading and Richards, 1994). After crossing a zone of down-to-the-basin normal faults farther down slope, the apron of wedge-shaped HAFs merges into a single large HAF (area Z, **Figure 5**). Specific features within the HAF are indistinct although amplitude variations are elongate (channels?) and define a textural trend that is parallel to the local direction of maximum gradient. The HAF narrows down slope until it is funneled through bathymetric highs to emerge and form the single large HAF of LE2 (**Figures 5**, **6**).

Sediment was supplied to LE2 through multiple entry points rather than through a single channel complex (**Figures 5**, **6**). No outer levees are observed anywhere along the transport path to or within LE2. Sediment was dispersed across the bulk of LE2 without leaving evidence for either a distributary channel system or branching (**Figure 6**) comparable to LE1. Instead, elongate textures are imaged in RMS amplitude extractions, most prominently defined by dark elongate features (low RMS values), in LE2 that vary in morphology in planform from lenticular or irregularly shaped to continuous with slightly convergent or slightly divergent margins (**Figure 6**). The most continuous

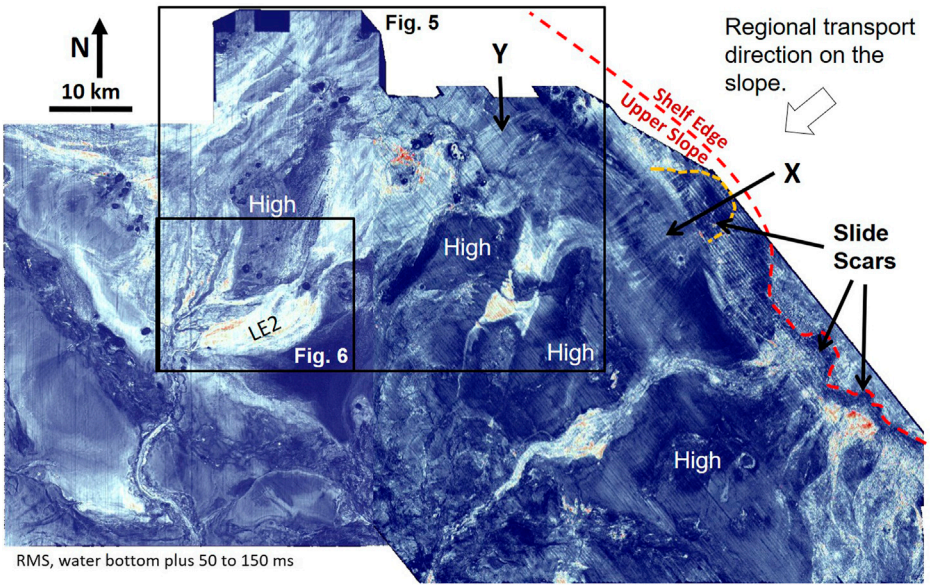

FIGURE 4 | A Root Mean Squared (RMS) amplitude extraction from 3D reflection seismic volumes on the middle to upper slope, off shore Nigeria (location in **Figure 1**). The image is calculated from the interval between 50 and 150 ms below seabed (approximately 100 m of sediment). Sediment transport is from northeast to southwest and water depth increases to the southwest. High RMS values are displayed as white to orange colors. The approximate position of the shelf edge is represented by a red dashed line. The edges of large slide complexes at the shelf edge are indicated by scallop-shaped indentations in the shelf edge. The edge of a large slide scar complex on the upper slope is indicated by an orange dashed line. Influential structural highs are annotated (High). The locations of panels 5, 6 are indicated. The location of LE2 is labeled as are the locations of areas X and Y (discussed in the text).

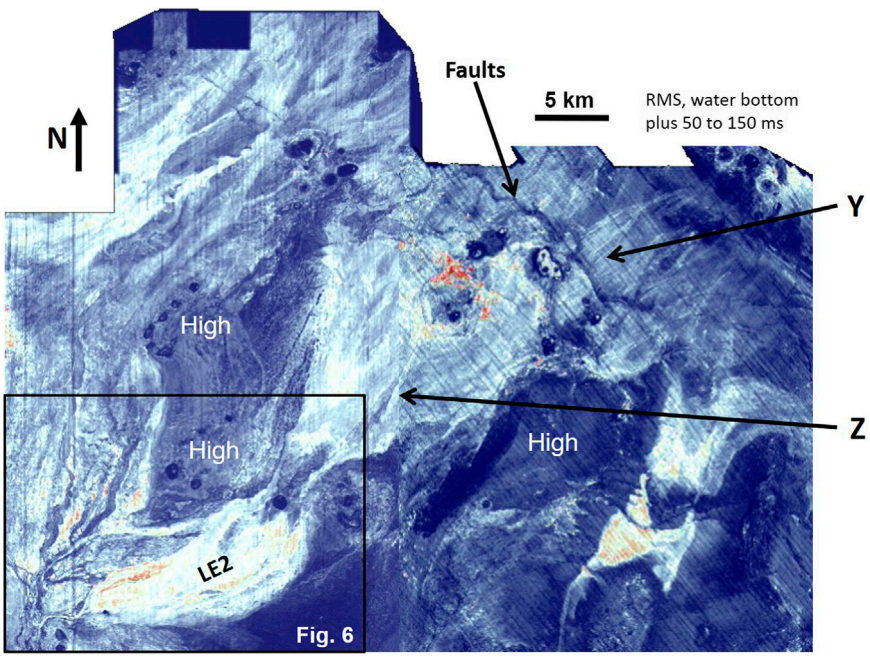

FIGURE 5 | A Root Mean Squared (RMS) amplitude extraction from two adjacent 3D reflection seismic volumes on the middle to upper slope, off shore Nigeria. See **Figure 4** for location. The image is calculated from the interval between 50 and 150 milliseconds (approximately 100 m of sediment) below seabed. High RMS values are displayed as white to orange colors. Sediment transport is from northeast to southwest. The location of panel 6 is indicated. Influential structural highs are annotated (High). The location of LE2 is labeled, as are the locations of areas Y and Z (discussed in the text).

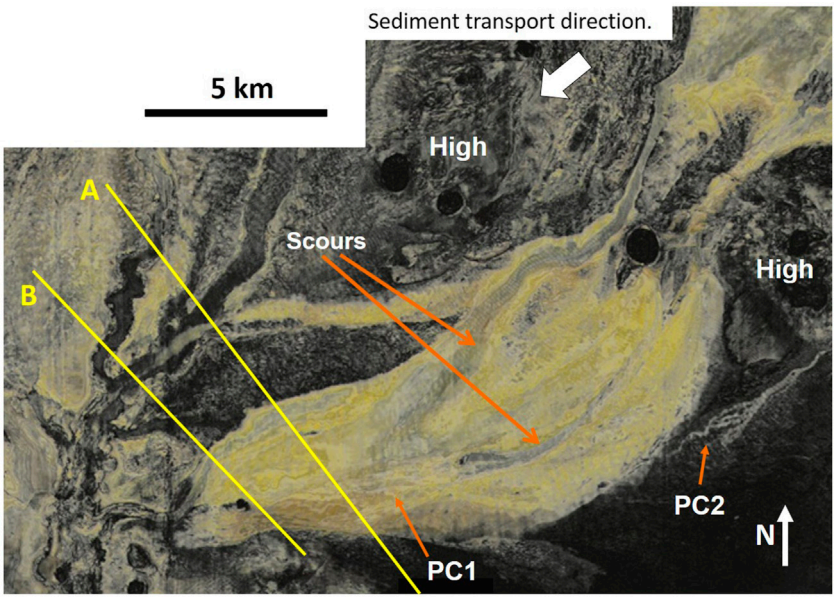

FIGURE 6 | A Root Mean Squared (RMS) amplitude extraction from a 3D reflection seismic volume on the middle slope, off shore Nigeria. See **Figures 4**, **5** for location. The image, which includes LE2, is calculated from the interval between 50 and 100 ms (approximately 50 m of sediment) below seabed. The sampled interval corresponds to the interval between blue lines in **Figure 7**. High RMS values are displayed as white to yellow colors. Sediment transport is from northeast to southwest. Dark, elongate, low sinuosity features with non-parallel sides, interpreted as scours within LE2, are labeled (Scours). Small possible channel forms may be seen locally within LE2 (PC1) as well as outside of LE2 (PC2). Influential structural highs are annotated (High). The locations of seismic cross sections in **Figure 7** are indicated by yellow lines labeled **(A)** and **(B)**.

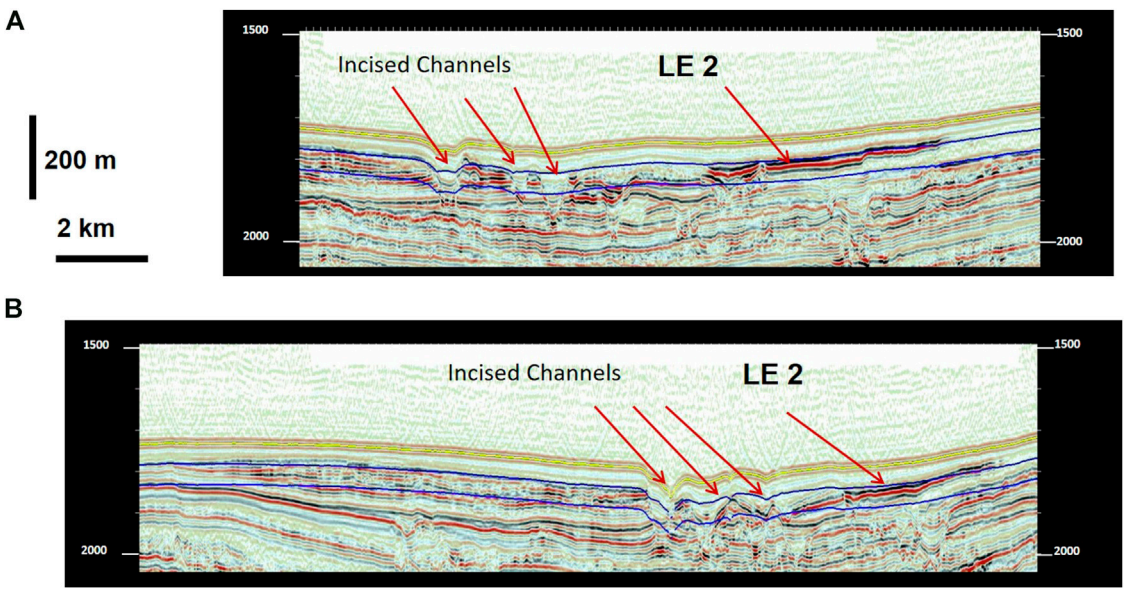

FIGURE 7 | Cross sections through LE2 from a 3D reflection seismic volume. See **Figure 6** for locations. The blue lines indicate the top and base of the interval from which the RMS (Root Mean Squared) values in **Figure 6** were calculated. **(A)** Seismic section through the distal portion of LE2. This portion of the lobate deposit is characterized by highly continuous reflections. Incisional bypass channels are evident to the west of LE2. **(B)** Seismic section through the terminus of LE2. LE2 continues to be characterized by a highly continuous reflection. The area to the west of LE2 is dominated by multiple incised channel.

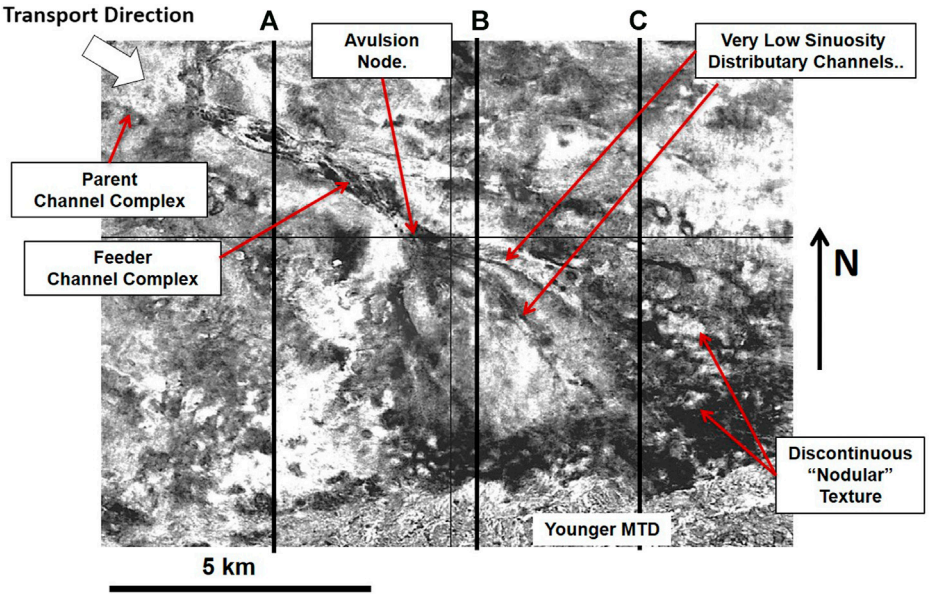

FIGURE 8 | A Root Mean Squared (RMS) amplitude extraction of LE3 from a 3D reflection seismic volume. The image is horizon referenced and derived from the interval 0–50 ms above the base of the lobate deposit (purple horizon in **Figure 9**). High RMS values are displayed as white color. Sediment transport is from northwest to southeast. The locations of seismic cross sections in **Figure 9** are indicated by vertical lines labeled **(A)**, **(B)** and **(C)**. Modified from Posamentier et al. (2000), Fowler et al. (2001), Posamentier and Kolla (2003), Saller et al. (2003), Saller et al. (2004), Ruzuar et al. (2005), Saller et al. (2008), and Saller et al. (2010).

elongate features lack the sharply defined parallel margins of channels that are clearly imaged in LE1 (**Figure 2**). A possible exception to the absence of conventional channels is present in the southern part of LE2 where a slightly divergent set of narrow moderately high amplitude threads (PC, **Figure 6**) appear locally down flow from a prominent elongate low amplitude feature.

At the down-flow terminus of LE2, deeply incised channels are observed (**Figures 6**, **7**). One is located at the terminus of the main part of LE2 (**Figure 7B**), while another is located at the terminus of a narrow arm of the HAF located to the west of LE2. These deeply incised channels are located at positions that would have, in combination, received any flows and transported sediments that bypassed LE2 (transient fan of Adeogba et al., 2005). These incised channels deepen along their path to the southwest and converge basinward with other erosional channels (**Figure 4**).

Lobate Example 3: A Channelized Lobate Deposit With Few Distributaries

Example 3 Regional Setting

LE3 (**Figure 8**) is located at the base of slope east of Kalimantan, Indonesia, in the Kutei Basin, Makassar Strait (**Figure 1B**). LE3 is part of a larger fan system on the basin floor, approximately 40 km from the shelf edge beneath about 2,000 m of water (Saller et al., 2008). Sediment transport generally was from west to east or southeast. The continental slope proximal to the fan that contains LE3 is irregular, including areas of both high and low gradient, as well as ridges that tend to stand above the regional slope profile. The stepped slope profile results from prominent toe thrusts that maintain a gradient of 2.1° at the base of slope compared to the basin floor gradient of 0.3° (Saller et al., 2004).

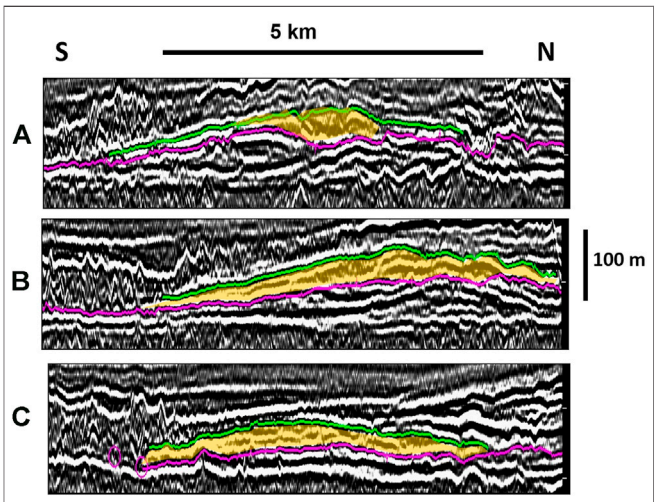

FIGURE 9 | Cross sections through LE3 from a 3D reflection seismic volume. See **Figure 8** for locations. The green and purple horizons indicate the top and base respectively of LE3 (highlighted in yellow). **(A)** Seismic section through the feeder channel complex of LE3. **(B)** Seismic section through the proximal part of LE3. **(C)** Seismic section through the distal part of LE3.

The fan, including LE3, has been imaged and interpreted multiple times (Posamentier et al., 2000; Fowler et al., 2001; Posamentier and Kolla, 2003; Saller et al., 2003; Saller et al., 2004; Ruzuar et al., 2005; Saller et al., 2008; Saller et al., 2010). The fan was deposited in association with a sea level lowstand about 240 ka (Saller et al., 2004). The submarine fan was both preceded

and followed immediately by substantial mass transport deposits (Posamentier et al., 2000; Fowler et al., 2001; Posamentier and Kolla, 2003; Saller et al., 2003; Saller et al., 2004; Ruzuar et al., 2005; Saller et al., 2008; Saller et al., 2010).

LE3 (**Figures 8**, **9**) is located approximately midway within a strongly progradational and moderately aggradational succession of lobate bodies (Saller et al., 2008). Each lobate body was connected to the same feeder channel-levee complex. Deposition, avulsion and abandonment of each lobate body resulted in the progressive basinward offset of successive lobate deposits and progradation of the system. The youngest expression of the channel-levee complex culminated with a terminal lobate deposit (Posamentier et al., 2000; Fowler et al., 2001; Posamentier and Kolla, 2003; Saller et al., 2003; Saller et al., 2004; Ruzuar et al., 2005; Saller et al., 2008; Saller et al., 2010). At least one mass transport complex (MTC) was deposited within the fan during progradation (Posamentier and Kolla, 2003; Saller et al., 2008) and a younger MTC eroded the southern edge of LE3 (**Figure 8**).

Example 3 Seismic Data

Images of LE3 are derived entirely from industry standard 3D reflection seismic data acquired in 1998–1999 by WesternGeco as part of the much larger Makassar 3D survey. The interpreted data have a dominant frequency of about 50 Hz (Saller et al., 2008) at the shallow depth of the studied fan. Assuming an acoustic velocity of 2,000 m/sec (Flood et al., 1997), the nominal vertical resolution of these data is approximately 10 m (**Table 1**). The plan view image provided in this paper is a horizon-referenced RMS amplitude display garnered from the uppermost 200 milliseconds (200 m) of data below the seabed. Bin spacing is 12.5 m by 12.5 m. The studied portion of the seismic volume extends from near the modern base of slope to a position approximately 22 km to the east on the basin floor.

Example 3 Description

LE3 is approximately 7 km wide, more than 7 km long, and a maximum of approximately 43 m thick near the proximal (NW) end of the lobate deposit yielding a width to thickness ratio of 163 (**Figures 8**, **9**; **Table 1**). LE3 is buried by approximately 160 m of mud-rich sediments. No core samples are available from LE3.

At the time of deposition, LE3 may have been a terminal lobe of the submarine fan (Posamentier and Kolla, 2003, their frontal splay). Alternatively, its single feeder channel complex (approximately 300–500 m wide) may have avulsed from a larger parent channel complex that extended into the basin as the fan prograded. Confinement of the parent channel complex was provided by a 110 m thick and 4,000 m wide outer levee (estimated from Posamentier and Kolla, 2003). The dimensions of the levee, if present, at the time of LE3 deposition are unknown.

The single feeder channel complex is about 5 km long between its connection to the larger parent channel complex and the apex of LE3 (**Figure 8**). The feeder complex appears to have been confined primarily by erosion although a contemporaneous levee cannot be discounted. Within the feeder channel, which is almost straight, smaller low sinuosity channel elements (sensu McHargue et al., 2011) are distinctly imaged. A branching point is present at the distal end of the feeder channel marking the proximal end of a small number of long distributary channels (up to 5 km long and 100–300 m wide) with very low sinuosity (**Figure 8**). No other branching points are recognized within LE3. No finer scale channel forms are recognizable surrounding the distributary channels or at the distal end of the distributaries. Fill within the distributary channels is too thin to image distinctly in cross-section (**Figure 9**).

Except for the few distributary channels, plan-view imaging of the sediment within LE3 ranges from featureless to nodular (**Figure 8**). The nodular features are particularly prominent around the fringe of LE3, but subtle variation within the main part of the lobate unit suggests that the nodular texture may be present throughout LE3. Nodular texture also is present lateral to LE3 in adjacent lobate bodies (**Figure 8**). Individual nodular features can be up to 200 m wide although a full range of smaller sizes, down to the resolution limit of the data, are evident.

In cross-section, LE3 is markedly lenticular (highlighted in yellow, **Figure 9**). It overlies multiple older lenticular lobate units and, at its distal part, is overlain by at least one lobate unit before burial by the channel-levee complex. The sediment within LE3 is crudely layered and imaged with moderate amplitudes. Compensational stacking of the successive older and younger lobate lenses is evident surrounding the proximal part of LE3 (**Figure 9**, sections A and B) but becomes more subtle distally as lens relief decreases (**Figure 9**, section C).

INTERPRETATION

Lobate Example 1 Interpretation

The diversity of amplitudes suggests that LE1 received flows transporting a wide range of grain-sizes including both sands and muds. The feeder channel complex and proximal distributary channels of LE1 are confined primarily by outer levees (**Figures 3B,C**). Low seismic RMS amplitudes in the levees suggest that they are composed dominantly of mud. Low seismic RMS amplitudes within outer levees contrast with high seismic RMS amplitudes within the feeder channel complex and within distributary channels of LE1. High RMS amplitudes require strong contrasts in impedance and suggest the presence of mixed sand and mud within the channel-fills. Farther down flow, where levees are no longer discernable, it is suspected that overbank sediments continue to have higher mud content relative to channel sediments accounting for distinct, well imaged channels. The presence of well-developed levees confining the feeder and proximal distributary channels, as well as the acoustic variability required to yield well imaged channels, suggests that the contributing flows were density stratified (Kneller and Buckee, 2000; Peakall et al., 2000; Hansen et al., 2015). As each turbidity current crossed LE1, the top of the dilute layer was eventually lost overbank by flow stripping as levee height decreased down flow.

At the terminus of each levee-confined distributary channel, instead of unchannelized deposits, a pervasively channelized unit is present that is dominated by a cluster of sub-parallel to slightly divergent small channels. Adjacent clusters tend to be laterally offset from each other suggesting compensation. LE1

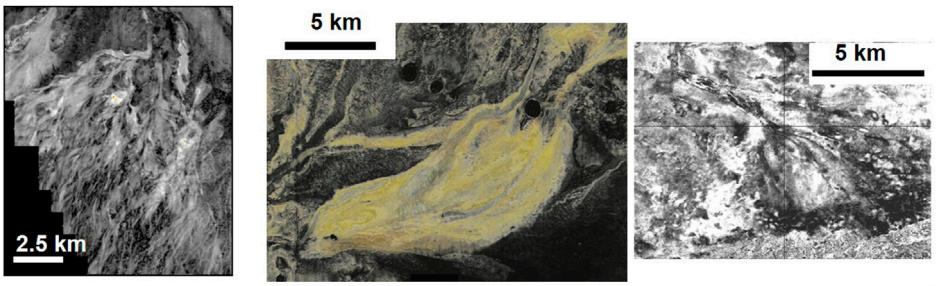

LE1: ***Pervasively channelized***
- Mud-rich stratified flows
- Single levee-confined feeder channel
- Extensive system of distributary channels
- Proximal distributaries are levee confined
- Many branching points
- Offset channel clusters suggest compensation
- Aspect ratio = 108

LE2: ***Unchannelized***
- Mud-poor stratified flows
- Fed by littoral drift
- Transport via multiple erosional gullies and channels
- Feeder channels lack any resolvable levees
- Elongate scours with non-parallel sides
- Deposition results from flow collapse
- Aspect ratio = 300

LE3***: Few long, straight distributaries***
- "Nodular" seismic character represents rafted blocks
- Few long, straight distributary channels
- Few branching points, mostly at the mouth of the feeder channel
- Deposition mostly from viscous flows
- Aspect ratio = 163

FIGURE 10 | Summary of distinctive characteristics of the three discussed lobate examples. See **Figures 2**, **6**, **8** for explanations of seismic RMS amplitude displays.

(**Figures 2**, **10**) is covered by distributary channels with numerous branching points, an observation that, when combined with the presence of levee-confined distributaries, is compatible with the proposal of Mulder and Etienne (2010) that lobate deposits with a well-developed distributary channel system appear to be constructed from relatively mud-rich flows. However, even their model for channelized lobes does not illustrate the high density of distributary channels present across all of LE1 (**Figures 2**, **10**).

Summary

In summary, LE1 is interpreted to have a well-developed distributary channel system that is interpreted to display the following characteristics (**Figures 10**, **11**):

1) Sediments were delivered to LE1 through a single levee-confined feeder channel complex.
2) Transported sediments were heterolithic, including enough mud in the upper dilute portion of flows to allow for outer levee construction.
3) Sediments were dispersed across LE1 via an extensive system of distributary channels.
4) The proximal distributary channels are interpreted to have been levee confined.
5) LE1 grew as a result of avulsions or bifurcations at numerous and diverse branching points along the distributary channel pathways.
6) The most distal visible channels form channel clusters that tend to be laterally offset relative to one another in a stacking pattern that suggests compensation.

Lobate Example 2 Interpretation

LE2 (**Figures 6**, **10**) appears to have only sparse, fine-scale distributary channels and a much higher aspect ratio (300) than LE1 (108) (**Table 1**). Much can be inferred regarding the nature of the shelf edge and slope from the regional horizon-based RMS amplitude extraction (**Figure 4**). The sizes, shapes and linkages of the HAFs displayed on the continental slope indicate the locations of sediment transport paths and deposition. The presence of high amplitudes (light colors in **Figure 4** through **Figure 6**) within the HAFs suggests sand-rich sediments within the HAFs (Posamentier and Kolla, 2003). The source area on the shelf for the sediment within LE2 lies outside the available seismic coverage. However, the transport path from shelf to lobate deposits is well imaged for sediment immediately to the east (area X in **Figure 4**). Upper slope architectures are very similar in areas X and Y so, by analogy, we interpret that those similar conditions prevailed for both systems at the shelf edge. No submarine canyon is imaged at or near the shelf edge up slope from area X. Instead, arcuate indentations in the shelf edge and upper slope are well imaged and are interpreted as coalesced slide scars (**Figure 4**). Because these slide scars are well imaged, we infer that submarine canyons, if present, also would be imaged. The narrow and linear HAFs immediately down slope of the slide scars (area X in **Figure 4**) are interpreted to represent numerous slope gullies, some of which terminate in small fan-shaped deposits. Others coalesce and continue down slope to deliver sediment to large HAFs. Because of the spatial association of slide scars and the clustered transport paths (**Figure 4**), it is

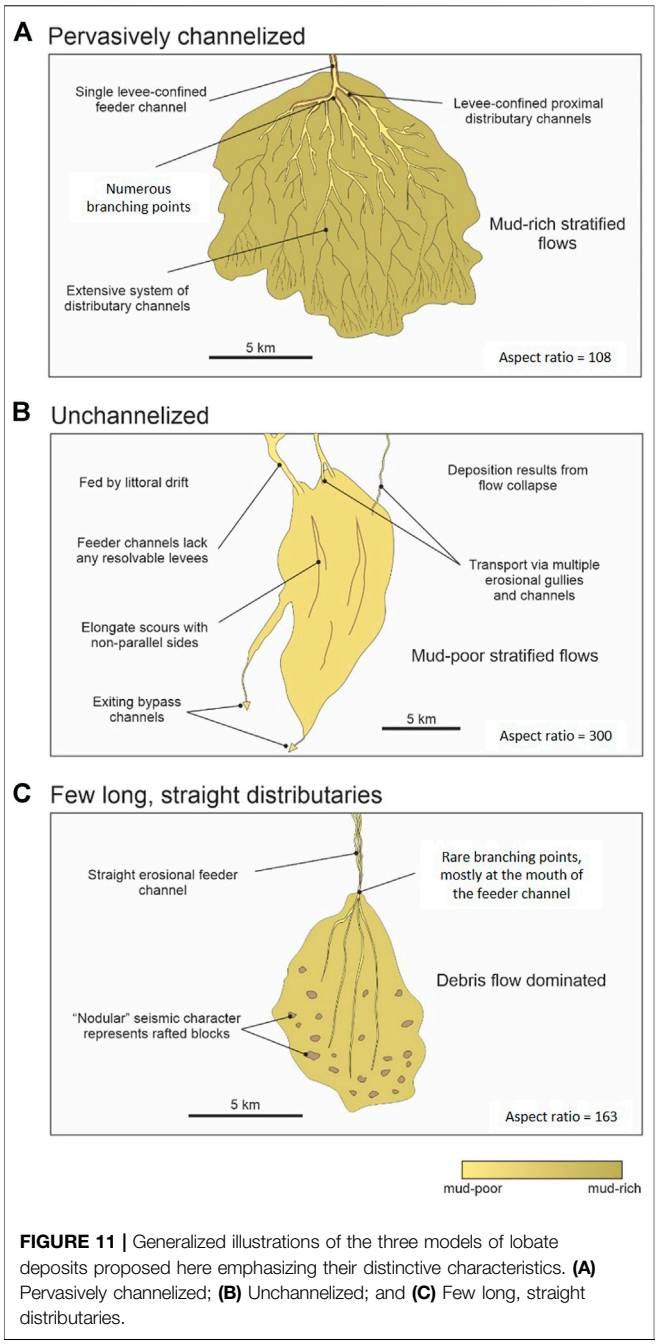

FIGURE 11 | Generalized illustrations of the three models of lobate deposits proposed here emphasizing their distinctive characteristics. **(A)** Pervasively channelized; **(B)** Unchannelized; and **(C)** Few long, straight distributaries.

inferred that the slide scars were integral to intercepting shelf sediments and directing them down slope within density currents. The gullies in area Y (**Figures 4**, **5**) up slope of LE2 have very similar morphology and clustering as in area X and, assuming lateral continuity of the slide scar pattern, are inferred to have the same origin as those in area X. Therefore, although a degree of speculation is required, features in area Y are interpreted to represent the transport path of shelf sediments that were intercepted at slide scars and directed through multiple HAFs to LE2.

We speculate that the dominant source of sediment was from littoral drift. The Niger Delta is a wave-dominated system today (Allen, 1965; Doust and Omatsola, 1990) with strong littoral cells (Burke, 1972; Biscara et al., 2013). Because littoral drift potentially is available all along the lowstand delta front, especially concentrated where slide scars intersect the shelf edge, it seems reasonable that gravity flows, consisting of sand-rich littoral deposits (Imhansoloeva et al., 2011), spilled over the indented lowstand shelf edge and traversed numerous gullies to coalesce in areas of decreased gradient as HAFs. No outer levees are observable anywhere within LE2, or along the train of HAFs leading to LE2, suggesting that the gravity flows that traversed the HAFs lacked sufficient mud caliber sediments to build outer levees (Posamentier and Kolla, 2003). Furthermore, these observations are consistent with the contention that the HAFs contain sand-rich sediment that originated from littoral drift on the shelf.

On LE2 (**Figure 6**), no large conventional distributary channels with parallel margins are observed. Instead, indistinct elongate textures are recorded by RMS amplitudes within LE2 (**Figure 6**). Some of the most continuous elongate features are slightly darker (lower RMS amplitude) than the surrounding deposits. Perhaps this amplitude distribution results from thinning of the sand-prone deposits within the linear features as a result of scouring reminiscent of the central feature of the Navy Fan (Carvajal et al., 2017). We further suggest that these elongate features served as conduits for sediment transport (De Leeuw et al., 2016; Ferguson et al., 2020). A possible exception occurs in a local area in the southern part of LE2 where fine-scale thread-like features (possible channels) appear to emanate from the distal end of one of the dark, elongate, linear features (PC1 in **Figure 6**). If these features are channels, analogous to the small channel threads to the east outside of LE2 (PC2 in **Figure 6**) they are markedly smaller than the channels in LE1. The origin of the possible fine-scale channels is unclear; they may be superficial, but they do demonstrate that channels, even fine-scale channels, when present, may be imaged successfully.

Deeply-incised channels at the terminus of LE2 deepen along their path to the southwest (**Figure 7**) and converge with other erosional channels (**Figure 4**). The strongly erosive character of these channels indicates that significant volumes of sediment periodically bypassed LE2 resulting in increased basal shear stress and scour (Adeogba et al., 2005; Gamberi and Rovere, 2011; Maier et al., 2011; Barton, 2012; Maier et al., 2012; Prather et al., 2012a; Maier et al., 2013; Yang and Kim, 2014). We reconcile these observations and the interpretation of sand-rich flows by speculating that deposition of LE2 occurred as flows slowed and collapsed at an area of relatively low gradient. Other flows had sufficient momentum to scour and bypass LE2 producing local erosion of linear troughs and incisional bypass-dominated channels. Compatible with this model, the dark, linear features are thought to have low RMS amplitude due to thinning or complete removal of sand by scour of more energetic flows.

Summary

LE2 is interpreted to have no conventional distributary channel system; rather it is interpreted to display, the following characteristics (**Figures 10**, **11**; **Table 1**):

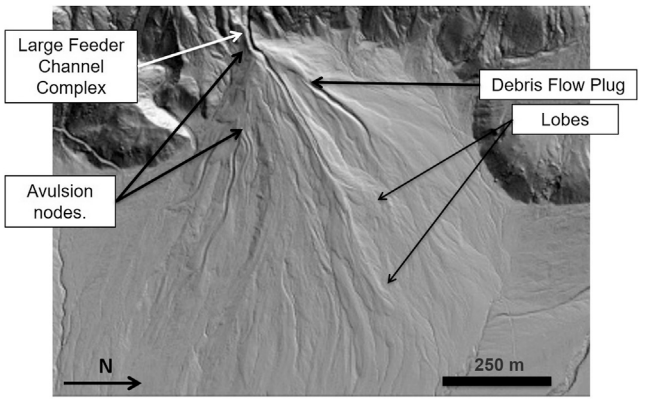

FIGURE 12 | Hill-shade map based on LiDAR produced topography of subaerial debris flow dominated fan in Saline Valley, California. Laminar flow of the subaerial debris flows has produced a surface distributary texture with long, nearly straight channels, sparse branching points, and narrow depositional bodies. This distributive architecture is reminiscent of LE3 (**Figure 8**). Source: Earthscope Eastern and Southern California. Resolution = 0.5 m. Lat. 36.824674°, Long. -117.919470°. The material for this example is based on services provided to the Plate Boundary Observatory by NCALM (http://www.ncalm.org). The Plate Boundary Observatory is operated by UNAVCO for EarthScope (http://www.earthscope.org) and supported by the National Science Foundation (No. EAR-0350028 and EAR-0732947).

1) LE2 likely is constructed of sediments derived from multiple points along the shelf edge (a line source) without evidence of a submarine canyon (a point source).
2) Transported sediments are interpreted to consist of mud-poor sandy littoral drift intercepted and remobilized at slide scars at or near the shelf edge.
3) The delivered sediments are transported from the shelf edge to LE2 via multiple erosional gullies or channels that are focused by slope topography toward the location of LE2.
4) Feeder channels and lobate deposits lack any resolvable levees suggesting that the delivered sediments are extremely sand-rich with minimal accompanying mud.
5) Large elongate scours with non-parallel sides are interpreted to be present.
6) No conventional distributary channel system is visible within the lobate deposit. Local thin threads (PC1 in **Figure 6**) near the southern margin may represent local distributaries.
7) Deposition is interpreted to result from collapse of sand-rich flows at decreased gradient although other, more robust flows scoured the deposits and bypassed LE2.

Lobate Example 3 Interpretation

LE3 (**Figures 8**, **10**) displays only a few distributaries that diverge at the mouth of the feeder channel and extend without further branching points to the observed limits of the lobate deposit. The absence of secondary branching points and secondary distributaries coupled with the very low sinuosity of the primary distributaries is distinctive. The nodular texture of seismic RMS amplitudes, best displayed in planform (**Figure 8**), are interpreted to be rafted coherent to semi-coherent blocks of allocthonous sediment within a surrounding mass of mud-rich sediment (e.g., Saller et al., 2008; Hodgson et al., 2016) and suggests the presence of abundant debrites. LE3 is crudely layered in cross-section (**Figure 9**) suggesting that multiple events are present. The fact that distributary channels and small nodular features are imaged suggests that secondary distributaries, if present, would be recognized in these data. The nodular texture, lack of observed secondary distributary channels, and the extremely low sinuosity of the primary distributary channels, are interpreted to result from deposition from viscous flows.

Interestingly, similar morphology of long, nearly straight distributary channels with few branching points, is well demonstrated for debris-flow dominated alluvial fans (**Figure 12**). In these alluvial fans, avulsion is triggered either by debris plugs and/or slow aggradation that fill the channel, or by unusually large events (De Haas et al., 2019); these mechanisms might apply to submarine systems as well.

Summary

LE3 is interpreted to have a small number of straight distributary channels and rare branching points (**Figures 10**, **11**; **Table 1**), and is interpreted to display the following characteristics:

1) LE3 is located at the end of a straight, erosional conduit without discernible levees and with minor slightly sinuous channel elements within its fill.
2) It displays a prominent "nodular" seismic character in plan view, typical of debrites, with individual nodular seismic features interpreted to represent rafted blocks up to 200 m wide.
3) A small number of long, straight distributary channels diverge at the mouth of the feeder channel.
4) Distributaries extend without further branching to near the end of the lobate deposit.
5) The long, straight, non-branching channels are interpreted to result primarily from viscous flows (debris flows) although minor turbidite and hybrid event deposits also could be present.

DISCUSSION

Processes and Sediment Caliber

The three lobate examples illustrated here are visually distinct based on distributary architecture (**Figures 10**, **11**). No core material is available from any of the three examples so interpretations of process and sediment caliber are conjectural, constrained by regional context, seismic response and depositional architecture (**Figures 10**, **11**). Based on these observations, we propose that relatively mud-rich turbulent, density-stratified flows produce levee-confined feeder channels, leveed proximal distributaries, and multiple secondary and tertiary distributaries with many branching points (LE1, **Figures 2**, **3**, **10**). Mud-poor turbidity currents, likely sourced from littoral drift, or via effective filtering of mud through flow stripping in long slope conduits (e.g., McHargue et al., 2011; Hodgson et al., 2016), are prone to collapse and result in a lobate

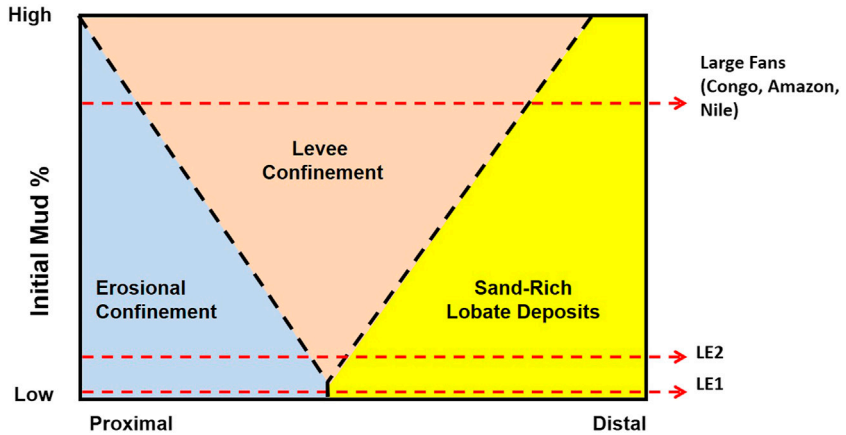

FIGURE 13 | Simplified schematic field diagram of the gross architectural succession from proximal to distal of a submarine turbidite system as a function of the abundance of initial mud in the average turbulent flow. Boundaries between fields are displayed as a linear function for simplicity but we acknowledge that these boundaries may be non-linear. The model is scale independent. Gradient is not considered here explicitly because mud-rich systems respond to gradient very differently than sand-rich systems. Mud is assumed to be located primarily in the upper dilute portion of highly stratified turbulent flows and to be consumed during transport primarily due to levee construction that shortens flow height. Levees decrease in height and decrease contribution to confinement down flow. Substrate entrainment is not considered. Also, this model does not consider the contribution of debris flows (LE3 does not apply). This model illustrates that systems with relatively high initial volumes of mud (higher on the Y axis) extend farther into the basin (more efficient) and tend to have larger sediment volume, larger levee volume, and more extensive levee-confined distributaries. Systems with relatively low initial volumes of mud (lower on the Y axis) extend a shorter distance into the basin (less efficient) and tend to have smaller sediment volume, smaller levee volume, increased reliance on erosional confinement, increased tendency to collapse, and increased sensitivity to gradient. Mud-rich systems, such as the Amazon, Nile or Congo Fans, are dominated by large levee-confined channels arranged in a distributary pattern. Extremely sand-rich systems, such as LE2 and Lobe X, are small, fed by erosional feeder channels with little to no distributary channels.

deposit with scour features but no distributaries (LE2, **Figure 4** through **Figures 7**, **10**). Debris flow-dominated lobate features display straight, erosional feeder channels, a small number of straight distributary channels emanating from the mouth of the feeder channel, and few branching points (LE3, **Figures 8**–**10**).

Interpretations of LE1 and LE2 are consistent with the suggestions of Mulder and Etienne (2010). Although their proposal is intended to explain morphologically distinct portions within a single lobate deposit, we extrapolate their process-response model and the concept of flow efficiency proposed by Mutti and Normark (1987) to illustrate the relationship between the mud-richness of contributing flows and the relative size and runout distance of lobate deposits (**Figure 13**). Consistent with this model, the implications of varying mud-richness in fluvial versus littoral drift sediment supply on the size and runout distance of lobate deposits have been documented by Paumard et al. (2020). In addition, we propose that mud-poor flows produce poorly channelized lobate deposits whereas mud-rich stratified flows produce lobate deposits with a prominent distributary channel network (**Figures 10**, **11**). Likewise, we suggest that the mode of feeder channel confinement serves as a useful proxy for sediment caliber: i.e., a levee-confined feeder channel implies mud-rich flows whereas erosionally-confined feeder channels without levees imply mud-poor flows.

Consistent with this proposal, LE1 displays a levee-confined feeder channel and an extensive system of distributary channels; in fact, except for its small size, LE1 has the morphology of a submarine fan (Normark, 1970). The volume of mud in a succession of mud-rich stratified flows feeds an increase in the volume and length of levees around the feeder channel as well as distributary channels (**Figure 13**). This trend is one of the drivers for progradation of the lobate body (Ferguson et al., 2020). At some undefined size, the mud-rich lobate deposit is large enough to be called a submarine fan containing multiple subordinate lobate deposits, one at the terminus of each levee-confined distributary.

The LE2 feeder system lacks levees and LE2 does not display conventional distributary channels, only scours (**Figure 13**). In mud-poor sediments, cohesion is minimal and these sediments are easily scoured (e.g., Hir et al., 2008). Although initial erosion of the substrate may be a prerequisite for channel initiation (Fildani et al., 2013; De Leeuw et al., 2016), parallel sided channels did not form in LE2; consistent with features generated in non-cohesive sediments in flumes (e.g., Metivier et al., 2005, their Figure 2; and Cantelli et al., 2011, their Figures 1, 4) and with the conclusion of Rowland et al. (2010) that cohesive banks are necessary to produce parallel sided channels in flume experiments.

The morphology of LE3, the straight erosional feeder channel and sparse straight distributaries without secondary branches, is visually similar to elongate non-branching features produced in physical experiments from viscous flows, or at most weakly turbulent flows (Fernandez et al., 2014). Alfaro et al., 2014, their Figure 19) illustrated a lobate feature on the Caribbean margin of Colombia with characteristics similar to LE3 that they interpreted to consist of mixed slumps, debrites and turbidites, consistent with our interpretation of LE3.

For the three examples studied here (**Table 1**), relatively mud-rich turbulent flows, LE1, produce a thick deposit relative to

width (W/T = 108) whereas the collapse of sand-rich flows, LE2, produces a thin deposit (W/T = 300). The debris flow dominated deposit, LE3, displays intermediate dimensions and an intermediate aspect ratio (W/T = 163). The significance of differences in aspect ratios between the three lobate examples is unclear but likely is linked to the dominant depositional process. Furthermore, there are implications for source-to-sink investigations on the size, morphology, and runout distance of lobate deposits, which we interpret to be influenced by the varying character of sediment supplied by fluvial versus littoral drift systems. However, more lithological data from contemporary systems, where the source material and physiography are well constrained, are needed to test these controls on the architecture of lobate deposits in deep-water systems.

Seismicly Imaged Subsurface and Modern Analogs

High resolution reflection seismic data of features at or near the seabed provide the most robust constraints on the 3D architecture of submarine lobate bodies. However, with few exceptions (e.g., Migeon et al., 2010; Jobe et al., 2017), core samples are sparse to non-existent. Additionally, because of resolution limitations, imaging of submarine lobes often reveals few details of architectural features within the lobe or even on the lobe surface. These fine-scale features are best revealed by high resolution bathymetric surveys (Maier et al., 2011; Carvajal et al., 2017; Maier et al., 2018; Droz et al., 2020; Maier et al., 2020). Such high resolution surveys illustrate the diversity of deep-water depositional systems but these surveys are rare. Given the relative sparsity of high resolution data on lobate deposits, it remains unclear whether the three examples shown here are representative of most such deposits. More data will help address this question.

In some cases, lens-shaped lobate deposits (**Figure 9**), typically stacked in a compensating pattern (*sensu* Mutti and Sonnino, 1981), can be recognized within a fan from reflection seismic data (e.g., Saller et al., 2008; Yang and Kim, 2014), but even these gross features may not be resolved unless near the seabed (e.g., Gervais et al., 2006; Deptuck et al., 2008; Bourget et al., 2010; Picot et al., 2016; Dennielou et al., 2017; Hamilton et al., 2017; Jobe et al., 2017).

Unambiguous images of distributary channel systems, as seen in LE1, have been recorded in some near surface seismic volumes of individual lobate deposits (Kidd, 1999; Posamentier and Kolla, 2003; Hadler-Jacobsen et al., 2005; Clark and McHargue, 2007; Hadler-Jacobsen et al., 2007; Prather et al., 2012b; Bakke et al., 2013; Oluboyo et al., 2014), or in high resolution bathymetric data (Maier et al., 2018). Curiously, in these examples, distributary channels tend to extend across the entire lobate body rather than just in the proximal portion. More common are lobate deposits with elongate to slightly divergent textures that might, ambiguously, be interpreted to represent distributaries (e.g., Jegou et al., 2008; Shanmugam et al., 2009; Bourget et al., 2010; Migeon et al., 2010; Sylvester et al., 2012; Egawa et al., 2013; Paumard et al., 2020).

If distributaries are not imaged, is that because they are present but difficult to image or because they are absent? Lobate deposits typically represent sand-rich environments both within and surrounding distributary channels. Therefore, it may be common that the acoustic properties of the channel fill are similar to those of surrounding overbank deposits. With little impedance contrast, imaging of distributaries is poor. Yet, in LE1 (**Figure 2**), distributaries are well imaged. Relatively mud-rich flows allowed for levee construction in proximal distributaries but also may have provided sufficient mud in overbank deposits of the middle to outer distributaries to provide impedance differentiation.

Distributaries may be present, even if not imaged, but it does not follow that one can assume their presence. For example, Lobe X of Prather et al. (2012a), Jobe et al. (2014), and Jobe et al. (2017) is located approximately 60 km to the northwest of LE1 and buried to a similar depth. Likewise, seismic data from Lobe X (60 Hz, 12.5 m × 18.75 m bin spacing) is very similar in resolution to LE1 data (**Figures 2**, **3**; **Table 1**). Multiple cores from Lobe X confirm that it is very sand-rich. However, in contrast to LE1, Lobe X displays neither levees nor distributaries. In that respect, it is similar to LE2.

Lobate deposits dominated by debrites, as in LE3 (**Figure 8**), have been imaged with sidescan data and confirmed with core from the Mississippi (Twichell et al., 1992; Twichell et al., 2009) and Nile (Ducassou et al., 2009; Migeon et al., 2010) submarine fans. However, given the very different tools with which these lobate bodies have been imaged versus LE3, the architecture is hard to compare. Nevertheless, these examples suggest that debrite dominated lobate deposits may be widespread.

Outcrop Analogs

We do not confidently recognize any outcrop analogs for any of the three examples of lobate deposits described here, although some partial analogs are suggested. It is challenging to reconcile architectural features illustrated in 3D reflection seismic data, even relatively high resolution data, with observations from outcrops because of poor resolution of seismic data relative to outcrop exposures and limited 3D exposure of even the best outcrops. Yet outcrop exposures are the principal way by which facies relationships within submarine lobate deposits are observed and documented.

An outcrop dominated by debrites, such as LE3 (**Figures 8**, **10**), may not be recognized as a lobate deposit. Likewise, channels are so numerous in LE1 that, in outcrop, it might not be recognized as a lobate deposit. An extensively channelized distributary system has been recognized in outcrop in the Brushy Canyon Formation in the form of multiple erosional channels that diverge at an acute angle (Carr and Gardner, 2000; Gardner et al., 2003). Erosional distributary channels have been interpreted from 2D exposures of the Kaza Formation of the Windermere Group (Terlaky et al., 2016). However, channel density in the Kaza Formation apparently is inadequate to match that of LE1. In the Ross Formation of Ireland, feeder channels and incisional transient fan channels have been recognized and mapped, but not distributaries within lobes

(Elliott, 2000; MacDonald et al., 2011; Pyles et al., 2014; Pierce et al., 2018).

Likewise, in the Skoorsteenberg Formation of South Africa, probably the most extensively exposed lobate succession in the world, a distributary system is not recognized, at least not as conventional erosional channels (Hodgetts et al., 2004; Hodgson et al., 2006). The multiple feeder channels of the Ongeluks River outcrop of the Skoorsteenberg Formation might be considered proximal distributaries although they are absent in the rest of the outcrop belt (Johnson et al., 2001; Hodgetts et al., 2004; Hodgson et al., 2006). Instead, what are seen repeatedly within lobate deposits of the Skoorsteenberg Formation are scours and zones of bed amalgamation (Johnson et al., 2001; Hodgetts et al., 2004; Hodgson et al., 2006; Prélat et al., 2010; Hofstra et al., 2015). The lack of distinct channels can be compared to LE2 (**Figures 6**, **10**), but there are few distinct features in LE2 to provide constraints.

Zones of bed amalgamation have been interpreted in the Skoorsteenberg Formation to represent the axes of distributive flows (depositional channels of Johnson et al., 2001). It is logical that zones of amalgamation represent locations of focused flow, and it is possible that these zones are present in a distributary pattern. Unfortunately, extensive work on these outcrops has not confirmed any particular pattern in map view (Hodgetts et al., 2004; Hodgson et al., 2006; Prélat et al., 2009). Also, it seems unlikely that the slight difference in the amount of mud within the preserved interbedded mud laminations of non-amalgamated areas versus zones of amalgamation would provide sufficient acoustic contrast to produce a channel image with distinct channel margins as displayed in reflection seismic images of LE1 (**Figure 2**).

Scours and zones of amalgamation also are common in other well exposed lobate deposits (e.g., Carr and Gardner, 2000; Elliott, 2000; Gardner et al., 2003; Remacha et al., 2005; MacDonald et al., 2011; Van der Merwe et al., 2014). In these systems, scours, or megaflutes, are interpreted to be local features rather than through going distributary channels (Elliott, 2000; Hodgson et al., 2006; MacDonald et al., 2011; Hofstra et al., 2016), although scours and scour trains (cyclic steps) have been proposed as possible channel precursors (Fildani et al., 2006; Maier et al., 2011; Armitage et al., 2012; Fildani et al., 2013; Maier et al., 2013; Covault et al., 2014; Covault et al., 2017).

Despite these challenges in determining the presence, absence, and distribution of distributaries in outcrop exposures, published illustrations of proposed models of unconfined units in outcrop routinely illustrate a few distributaries in the proximal lobe and none in the middle and distal lobe (e.g., Hirayama and Nakajima, 1977; Eschard et al., 2004; Hodgson, 2009; Prélat et al., 2010; Bernhardt et al., 2011; MacDonald et al., 2011; Brunt et al., 2013; Etienne et al., 2013; So et al., 2013; Grundvåg et al., 2014; Van der Merwe et al., 2014; Masalimova et al., 2016; Terlaky et al., 2016; Kane et al., 2017).

Classification

Normark (1970), Mutti and Ghibaudo (1972), and Normark (1978) loosely defined a lobe as part of a submarine fan consisting of a lobate sand-rich deposit at the distal end of a feeder channel and containing a distributary channel system in its proximal part. However, lobate depositional bodies can be present at multiple scales with a variety of architectures and permeability structures. For flexibility, it seems advisable to use a broader definition of the term lobe and differentiate diverse architectures with a standardized set of descriptors such as "pervasively channelized lobe" or "unchannelized lobe." This approach is flexible and can be adapted as new architectures are recognized. We are fully aware that the term "lobe" has been used to label a specific level within a hierarchy of lobate architectures (Prélat et al., 2009; Groenenberg et al., 2010; Mulder and Etienne, 2010; Prélat and Hodgson, 2013) defined by an empirical range of two-dimensional external dimensions (Prélat et al., 2009). We note that using a general and common morphological term such as lobe to describe one particular scale within a hierarchy of lobate bodies can cause confusion.

Hierarchy

The outcrop belt of lobate deposits that is most intensely studied and extensively exposed is the Skoorsteenberg Formation in the Tanqua Karoo Basin, South Africa (e.g., Johnson et al., 2001; Hodgson et al., 2006; Prélat et al., 2009; Groenenberg et al., 2010; Prélat and Hodgson, 2013). These deposits have been interpreted to display a hierarchy of tabular, lobate sandstone bodies that systematically increase in thickness and lateral extent with increasing rank. Furthermore, each higher rank within the sandstone hierarchy is separated by a siltstone unit that correspondingly also increases in thickness (Prélat et al., 2009), which is the fine-grained fringe of a body at the same hierarchical level (Prélat and Hodgson, 2013). This scheme has been adopted by other researchers for other lobate deposits (e.g., Mulder and Etienne, 2010; Grundvåg et al., 2014; Pierce et al., 2018).

Each unit within a hierarchical level is separated from the others by avulsion. A plan view map imaged by three-dimensional reflection seismic data is helpful for recognizing avulsions. However, it is difficult to assign a specific hierarchical term as defined by Prélat et al. (2009) based on reflection seismic data alone (i.e., without bed scale lithologic data) and thus it is not directly transferrable to the lobate units described here. Therefore, we choose to use the descriptive term "lobate" to refer to these seismically imaged examples.

LE1 Hierarchy

LE1 is a unit within a larger fan deposit (Prélat et al., 2010), suggesting that a hierarchical structure might be present. However, within LE 1 (**Figure 1**), many avulsions are imaged at many scales implying a large and unwieldy number of subordinate levels of hierarchy within the deposit. A distributary at one scale is a feeder channel at a finer scale and all lobate units, regardless of scale, are pervasively channelized. At multiple scales, each distributary channel avulses and feeds an additional cluster of distributary channels. Perhaps each channel cluster is analogous to a lobe in this case, or, an unchannelized and unresolved lobe is present at the distal end of each small distributary of each ultimate channel cluster. The latter option implies a very large number of strongly overlapping, unresolved, small lobes.

Perhaps, rather than a hierarchical architecture, LE1 has a fractal structure. Straub and Pyles (2012) provided a mechanism for testing hierarchical versus fractal structure with a modified compensational index. Unfortunately, this requires measurement of the thickness of all units at all scales and the vertical resolution of seismic profiles (**Figure 2**) of LE1 is inadequate for this purpose.

LE2 Hierarchy

LE2 is a solitary deposit, not a component of a larger submarine fan. Due to the absence of distributary channels and avulsions, the conventional basis for recognizing smaller hierarchical units within LE2 is lacking (**Figure 5**). Alternatively, because sediments enter LE2 from two entry points, the deposits derived from each entry point might form subunits within LE2. This setting is more likely to cause such subunits if the entry points were active at different times rather than simultaneously. Unfortunately, seismic resolution is inadequate to test this model. Interestingly, thin (meter scale) laterally offset lobate units within a potentially analogous deposit (Lobe X of Prather et al., 2012a; Jobe et al., 2017) have been confirmed with multiple cores. However, again, comparable lobate units, if present in LE2, are too thin to image with our available data.

LE3 Hierarchy

LE3 is a unit within a larger fan deposit (Saller et al., 2008), suggesting that a hierarchical structure might be present. The only recognized avulsion node of LE3 is located at the mouth of the feeder channel (**Figure 7**). The distributaries that diverge from that avulsion node might provide a basis for defining a hierarchy within LE3 if a separate lens of sediment is associated with each distributary. Unfortunately, no lense-shaped deposits are recognized unambiguously in cross-section within LE3 (**Figure 8**) perhaps due to limited vertical resolution. Consequently, the presence of an internal hierarchy within Lobate Example 3 remains speculative.

CONCLUSION

1) Three lobate examples (LE) presented here illustrate some diversity of lobate architectures and provide additional models to guide interpretation (**Figures 10**, **11**).
2) Although speculative, we suggest a conceptual model for the morphology of lobate deposits and their associated channels as products of specific processes and mud concentration (**Figures 10**–**12**).
3) LE1: Relatively mud-rich turbidity currents produce levee-confined feeder channels, levee-confined proximal distributaries, and multiple secondary and tertiary distributaries with many branching points (**Figure 11A**).
4) LE2: Mud-poor turbulent flows, likely sourced from littoral drift, are prone to collapse and result in a lobate deposit with scour features but no distributaries comparable to LE1 (**Figure 11B**).
5) LE3: Debris (viscous) flow dominated lobate features display straight, erosional feeder channels, a small number of straight distributary channels emanating from the mouth of the feeder channel, and minimal branching points (LE3, **Figure 11C**).
6) These lobate examples illustrate the important role of source material, basin margin physiography, and seabed topography in contolling the architecture of lobate features, and that these are important considerations in source-to-sink studies.
7) Outcrop analogs for the three lobate deposits described here are not obvious. For example, it is unclear if zones of amalgamation, which are common in outcrops of lobate deposits, will look like conventional channels or distributaries in horizon-referenced displays from 3D reflection seismic data or if they will be imaged at all.

DATA AVAILABILITY STATEMENT

The data analyzed in this study is subject to the following licenses/restrictions: The seismic data are petroleum company proprietary data to which we no longer have access. The illustrated images of seismic data are highly modified from previously published figures as referenced within the text. Requests to access these datasets should be directed to TM, timmchar@stanford.edu.

AUTHOR CONTRIBUTIONS

TM is the principal author and primary seismic interpreter. DH interpreted the seismic data of example 3 and contributed significantly to writing and editing the paper. ES contributed significantly to discussions of processes involved in the deposition of the three examples, contributed significantly to writing and editing the paper, proposed the subaerial analog and secured the alluvial fan image used in **Figure 13**.

ACKNOWLEDGMENTS

The authors would like to thank Chevron Nigeria Ltd. and the Nigerian National Petroleum Co. for permission to publish data for this research. An earlier version of this paper was greatly improved by the thorough review by S. A. Grundvåg and an anonymous reviewer. The current version greatly benefited from reviews by R. Tinterri and Y. T. Spychala. The research was supported through the Stanford Project on Deepwater Depositional Systems by AERA, Anadarko, Aramco Services Company, California Resources Corporation, Chevron, Conoco-Phillips, Hess, Nexen, Pemex, PTTEP, RAG, Schlumberger, Shell, Woodside, and YPF, and the Lobe 3 Joint Industry Project by AkerBP, BHP, BP, Equinor, Hess, Neptune Energy, Petrobras, Petrochina, Total, Vår Energi, and Woodside.

REFERENCES

Adeogba, A. A., McHargue, T. R., and Graham, S. A. (2005). Transient Fan Architecture and Depositional Controls from Near-Surface 3-D Seismic Data, Niger Delta continental Slope. *Bulletin* 89, 627–643. doi:10.1306/11200404025

Alfaro, E., Holz, M., and Holz, M. (2014). Seismic Geomorphological Analysis of deepwater Gravity-Driven Deposits on a Slope System of the Southern Colombian Caribbean Margin. *Mar. Pet. Geology.* 57, 294–311. doi:10.1016/j.marpetgeo.2014.06.002

Allen, J. R. L. (1965). Late Quaternary Niger Delta, and Adjacent Areas - Sedimentary Environments and Lithofacies. *Am. Assoc. Pet. Geologists Bull.* 49, 547–800.

Armitage, D. A., McHargue, T., Fildani, A., and Graham, S. A. (2012). Postavulsion Channel Evolution: Niger Delta continental Slope. *Bulletin* 96, 823–843. doi:10.1306/09131110189

Bakke, K., Kane, I. A., Martinsen, O. J., Petersen, S. A., Johansen, T. A., Hustoft, S., et al. (2013). Seismic Modeling in the Analysis of Deep-Water sandstone Termination Styles. *Bulletin* 97, 1395–1419. doi:10.1306/03041312069

Barton, M. D. (2012). "Evolution of an Intra-slope Apron, Offshore Niger Delta Slope: Impact of Step Geometry on Apron Architecture," in *Application of the Principles of Seismic Geomorphology to continental Slope and Base-Of-Slope Systems: Case Studies from Seafloor and Near-Seafloor Analogues*. Editors B. E. Prather, M. E. Deptuck, D. Mohrig, B. Van Hoorn, and R. B. Wynn (Tulsa, OK: SEPM Special Publication), 181–197. doi:10.2110/pec.12.99.0181

Beaubouef, R. T., Rossen, C., Zelt, F. B., Sullivan, M. D., Mohrig, D. C., and Jennette, D. C. (1999). "Deep-Water Sandstones, Brushy Canyon Formation, West Texas," in *AAPG Hedberg Field Research Conference* (Tulsa, Oklahoma, USA: American Association of Petroleum Geologists). doi:10.1306/ce40695

Bell, D., Kane, I. A., Pontén, A. S. M., Flint, S. S., Hodgson, D. M., and Barrett, B. J. (2018). Spatial Variability in Depositional Reservoir Quality of Deep-Water Channel-Fill and Lobe Deposits. *Mar. Pet. Geology.* 98, 97–115. doi:10.1016/j.marpetgeo.2018.07.023

Bernhardt, A., Jobe, Z. R., and Lowe, D. R. (2011). Stratigraphic Evolution of a Submarine Channel-Lobe Complex System in a Narrow Fairway within the Magallanes Foreland basin, Cerro Toro Formation, Southern Chile. *Mar. Pet. Geology.* 28, 785–806. doi:10.1016/j.marpetgeo.2010.05.013

Biscara, L., Mulder, T., Hanquiez, V., Marieu, V., Crespin, J.-P., Braccini, E., et al. (2013). Morphological Evolution of Cap Lopez Canyon (Gabon): Illustration of Lateral Migration Processes of a Submarine canyon. *Mar. Geology.* 340, 49–56. doi:10.1016/j.margeo.2013.04.014

Bonnel, C., Dennielou, B., Droz, L., Mulder, T., and Berné, S. (2005). Architecture and Depositional Pattern of the Rhône Neofan and Recent Gravity Activity in the Gulf of Lions (Western Mediterranean). *Mar. Pet. Geology.* 22, 827–843. doi:10.1016/j.marpetgeo.2005.03.003

Bourget, J., Zaragosi, S., Mulder, T., Schneider, J.-L., Garlan, T., Van Toer, A., et al. (2010). Hyperpycnal-fed Turbidite Lobe Architecture and Recent Sedimentary Processes: A Case Study from the Al Batha Turbidite System, Oman Margin. *Sediment. Geology.* 229, 144–159. doi:10.1016/j.sedgeo.2009.03.009

Brunt, R. L., Di Celma, C. N., Hodgson, D. M., Flint, S. S., Kavanagh, J. P., and van der Merwe, W. C. (2013). Driving a Channel through a Levee when the Levee Is High: An Outcrop Example of Submarine Down-Dip Entrenchment. *Mar. Pet. Geology.* 41, 134–145. doi:10.1016/j.marpetgeo.2012.02.016

Burke, K. (1972). Longshore Drift, Submarine Canyons, and Submarine Fans in Development of Niger Delta. *Am. Assoc. Pet. Geologists Bull.* 56, 1975–1983.

Cantelli, A., Pirmez, C., Johnson, S., and Parker, G. (2011). Morphodynamic and Stratigraphic Evolution of Self-Channelized Subaqueous Fans Emplaced by Turbidity Currents. *J. Sediment. Res.* 81, 233–247. doi:10.2110/jsr.2011.20

Carr, M., and Gardner, M. H. (2000). "Portrait of a Basinfloor Fan for sandy deepwater Systems, Permian Lower Brushy Canyon Formation, West Texas," in *Fine-grained Turbidite Systems*. Editors A. H. Bouma and C. G. Stone (American Association of Petroleum Geologists Memoir 72/SEPM Special Publication), 215–232.

Carvajal, C., Paull, C. K., Caress, D. W., Fildani, A., Lundsten, E., Anderson, K., et al. (2017). Unraveling the Channel-Lobe Transition Zone with High-Resolution AUV Bathymetry: Navy Fan, Offshore Baja California, Mexico. *J. Sediment. Res.* 87, 1049–1059. doi:10.2110/jsr.2017.58

Clark, J., and McHargue, T. (2007). *Stratigraphic and Spatial Changes in Channel Morphology Related to Deepwater Processes in Confined and Ponded Slope Mini-Basins, Angola*. Long Beach, California: American Association of Petroleum Geologists, AAPG Search and Discover Article #90063 AAPG Annual Convention.

Covault, J. A., Kostic, S., Paull, C. K., Ryan, H. F., and Fildani, A. (2014). Submarine Channel Initiation, Filling and Maintenance from Sea-Floor Geomorphology and Morphodynamic Modelling of Cyclic Steps. *Sedimentology* 61, 1031–1054. doi:10.1111/sed.12084

Covault, J. A., Kostic, S., Paull, C. K., Sylvester, Z., and Fildani, A. (2017). Cyclic Steps and Related Supercritical Bedforms: Building Blocks of Deep-Water Depositional Systems, Western North America. *Mar. Geology.* 393, 4–20. doi:10.1016/j.margeo.2016.12.009

Damuth, J. E. (1994). Neogene Gravity Tectonics and Depositional Processes on the Deep Niger Delta continental Margin. *Mar. Pet. Geology.* 11, 320–346. doi:10.1016/0264-8172(94)90053-1

De Leeuw, J., Eggenhuisen, J. T., and Cartigny, M. J. (2016). Morphodynamics of Submarine Channel Inception Revealed by New Experimental Approach. *Nat. Commun.* 7 (1), 1–7. doi:10.1038/ncomms10886

Dennielou, B., Droz, L., Babonneau, N., Jacq, C., Bonnel, C., Picot, M., et al. (2017). Morphology, Structure, Composition and Build-Up Processes of the Active Channel-Mouth Lobe Complex of the Congo Deep-Sea Fan with Inputs from Remotely Operated Underwater Vehicle (ROV) Multibeam and Video Surveys. *Deep Sea Res. Part Topical Stud. Oceanography* 142, 25–49. doi:10.1016/j.dsr2.2017.03.010

Dennielou, B., Jallet, L., Sultan, N., Jouet, G., Giresse, P., Voisset, M., et al. (2009). Post-glacial Persistence of Turbiditic Activity within the Rhône Deep-Sea Turbidite System (Gulf of Lions, Western Mediterranean): Linking the Outer Shelf and the basin Sedimentary Records. *Mar. Geology.* 257, 65–86. doi:10.1016/j.margeo.2008.10.013

Deptuck, M. E., Piper, D. J. W., Savoye, B., and Gervais, A. (2008). Dimensions and Architecture of Late Pleistocene Submarine Lobes off the Northern Margin of East Corsica. *Sedimentology* 55, 869–898. doi:10.1111/j.1365-3091.2007.00926.x

Doughty-Jones, G., Mayall, M., and Lonergan, L. (2017). Stratigraphy, Facies, and Evolution of Deep-Water Lobe Complexes within a Salt-Controlled Intraslope Minibasin. *Bulletin* 101, 1879–1904. doi:10.1306/01111716046

Doust, H., and Omatsola, E. (1990). "Niger Delta," in *Divergent/Passive Margin Basins*. Editors J. D. Edwards and P. A. Santagrossi (American Association of Petroleum Geologists Memoir), 201–238.

Droz, L., Jégou, I., Gillet, H., Dennielou, B., Bez, M., Canals, M., et al. (2020). On the Termination of Deep-Sea Fan Channels: Examples from the Rhône Fan (Gulf of Lion, Western Mediterranean Sea). *Geomorphology* 369, 107368. doi:10.1016/j.geomorph.2020.107368

Ducassou, E., Migeon, S. B., Mulder, T., Murat, A., Capotondi, L., Bernasconi, S. M., et al. (2009). Evolution of the Nile Deep-Sea Turbidite System during the Late Quaternary: Influence of Climate Change on Fan Sedimentation. *Sedimentology* 56, 2061–2090. doi:10.1111/j.1365-3091.2009.01070.x

Egawa, K., Furukawa, T., Saeki, T., Suzuki, K., and Narita, H. (2013). Three-dimensional Paleomorphologic Reconstruction and Turbidite Distribution Prediction Revealing a Pleistocene Confined basin System in the Northeast Nankai Trough Area. *Bulletin* 97, 781–798. doi:10.1306/10161212014

Elliott, T. (2000). "Depositional Architecture of a Sand-Rich, Channelized Turbidite System: The Upper Carboniferous Ross Sandstone Formation, Western Ireland," in *Deep-Water Reservoirs of the World*. Editors P. Weimer, R. M. Slatt, J. Coleman, N. C. Rossen, H. Nelson, A. H. Bouma, et al. Gulf Coast Section SEPM Foundation 20th Annual Research Conference, Houston, TX, 342–373. doi:10.5724/gcs.00.15.0342

Eschard, R., Albouy, E., Gaumet, F., and Ayub, A. (2004). Comparing the Depositional Architecture of basin Floor Fans and Slope Fans in the Pab Sandstone, Maastrichtian, Pakistan, *Geol. Soc. Lond. Spec. Publications* 222, 159–185. doi:10.1144/gsl.sp.2004.222.01.09

Etienne, S., Mulder, T., Razin, P., Bez, M., Désaubliaux, G., Joussiaume, R., et al. (2013). Proximal to Distal Turbiditic Sheet-Sand Heterogeneities: Characteristics of Associated Internal Channels. Examples from the Trois Evêchés Area, Eocene-Oligocene Annot Sandstones (Grès d'Annot), SE France. *Mar. Pet. Geology.* 41, 117–133. doi:10.1016/j.marpetgeo.2012.03.007

Ferguson, R. A., Kane, I. A., Eggenhuisen, J. T., Pohl, F., Tilston, M., Spychala, Y. T., et al. (2020). Entangled External and Internal Controls on Submarine Fan

Evolution: an Experimental Perspective. *Depositional Rec.* 6 (3), 605–624. doi:10.1002/dep2.109

Fernandez, R. L., Cantelli, A., Pirmez, C., Sequeiros, O., and Parker, G. (2014). Growth Patterns of Subaqueous Depositional Channel Lobe Systems Developed over A Basement with A Downdip Break in Slope: Laboratory Experiments. *J. Sediment. Res.* 84, 168–182. doi:10.2110/jsr.2014.10

Fildani, A., Hubbard, S. M., Covault, J. A., Maier, K. L., Romans, B. W., Traer, M., et al. (2013). Erosion at Inception of Deep-Sea Channels. *Mar. Pet. Geology.* 41, 48–61. doi:10.1016/j.marpetgeo.2012.03.006

Fildani, A., Normark, W. R., Kostic, S., and Parker, G. (2006). Channel Formation by Flow Stripping: Large-Scale Scour Features along the Monterey East Channel and Their Relation to Sediment Waves. *Sedimentology* 53, 1265–1287. doi:10.1111/j.1365-3091.2006.00812.x

Flood, R. D., Pirmez, C., and Yin, H. (1997). "The Compressional-Wave Velocity of Amazon Fan Sediments: Calculation from Petrophysical Properties and Variation with clay Content," in *Proceedings of the Ocean Drilling Project, Scientific Results 155*. R. D. Flood, D. J. W. Piper, A. Klaus, and L. C. Peterson (College Station, Texas: Ocean Drilling Program), 477–496.

Fowler, J. N., Guritno, E., Sherwood, P., and Smith, M. J. (2001). IPA01-G-120. Depositional Architectures of Recent Deep Water Deposits in the Kutei Basin, East Kalimantan. In Proceedings of the Annual Convention-Indonesian Petroleum Association (Jakarta, Indonesia: Indonesian Petroleum Association), 409–422.

Gamberi, F., and Rovere, M. (2011). Architecture of a Modern Transient Slope Fan (Villafranca Fan, Gioia basin-Southeastern Tyrrhenian Sea). *Sediment. Geology.* 236, 211–225. doi:10.1016/j.sedgeo.2011.01.007

Gardner, M. H., Borer, J. M., Melick, J. J., Mavilla, N., Dechesne, M., and Wagerle, R. N. (2003). Stratigraphic Process-Response Model for Submarine Channels and Related Features from Studies of Permian Brushy Canyon Outcrops, West Texas. *Mar. Pet. Geology* 20, 757–787. doi:10.1016/j.marpetgeo.2003.07.004

Gervais, A., Savoye, B., Mulder, T., and Gonthier, E. (2006). Sandy Modern Turbidite Lobes: A New Insight from High Resolution Seismic Data. *Mar. Pet. Geology* 23, 485–502. doi:10.1016/j.marpetgeo.2005.10.006

Gorsline, D. S., and Emery, K. O. (1959). Turbidity-current Deposits in San Pedro and Santa Monica Basins off Southern California. *Geol. Soc. America Bull.* 70, 279–290. doi:10.1130/0016-7606(1959)70[279:tdispa]2.0.co;2

Groenenberg, R. M., Hodgson, D. M., Prélat, A., Luthi, S. M., and Flint, S. S. (2010). Flow-Deposit Interaction in Submarine Lobes: Insights from Outcrop Observations and Realizations of a Process-Based Numerical Model. *J. Sediment. Res.* 80, 252–267. doi:10.2110/jsr.2010.028

Grundvåg, S.-A., Johannessen, E. P., Helland-Hansen, W., and Plink-Björklund, P. (2014). Depositional Architecture and Evolution of Progradationally Stacked Lobe Complexes in the Eocene Central Basin of Spitsbergen. *Sedimentology* 61, 535–569. doi:10.1111/sed.12067

Haas, T., Densmore, A. L., Hond, T., and Cox, N. J. (2019). Fan-Surface Evidence for Debris-Flow Avulsion Controls and Probabilities, Saline Valley, California. *J. Geophys. Res. Earth Surf.* 124, 1118–1138. doi:10.1029/2018jf004815

Hadler-Jacobsen, F., Gardner, M. H., and Borer, J. M. (2007). "Seismic Stratigraphic and Geomorphic Analysis of Deep-marine Deposition along the West African continental Margin," in *Seismic Geomorphology: Applications to Hydrocarbon Exploration and Production: London*. Editors R. J. Davies, H. W. Posamentier, L. J. Wood, and J. A. Cartwright (London: Geological Society Special Publication), 47–84. doi:10.1144/GSL.SP.2007.277.01.04

Hadler-Jacobsen, F., Johannessen, E. P., Ashton, N., Henriksen, S., Johnson, S. D., and Kristensen, J. B. (2005).January. Submarine Fan Morphology and Lithology Distribution: a Predictable Function of Sediment Delivery, Gross Shelf-To-basin Relief, Slope Gradient and basin Topography, *Geol. Soc. Lond. Pet. Geology. Conf. Ser.* 6, 1121–1145. doi:10.1144/0061121

Hamilton, P., Gaillot, G., Strom, K., Fedele, J., and Hoyal, D. (2017). Linking Hydraulic Properties in Supercritical Submarine Distributary Channels to Depositional-Lobe Geometry. *J. Sediment. Res.* 87, 935–950. doi:10.2110/jsr.2017.53

Hanquiez, V., Mulder, T., Toucanne, S., Lecroart, P., Bonnel, C., Marchès, E., et al. (2010). The sandy Channel-Lobe Depositional Systems in the Gulf of Cadiz: Gravity Processes Forced by Contour Current Processes. *Sediment. Geology.* 229, 110–123. doi:10.1016/j.sedgeo.2009.05.008

Hansen, L. A., Callow, R. H., Kane, I. A., Gamberi, F., Rovere, M., Cronin, B. T., et al. (2015). Genesis and Character of Thin-Bedded Turbidites Associated With Submarine Channels. *Marine Petrol. Geol.* 67, 852–879.

Hir, P. L., Cann, P., Waeles, B., Jestin, H., and Bassoullet, P. (2008). "Chapter 11 Erodibility of Natural Sediments: Experiments on Sand/mud Mixtures from Laboratory and Field Erosion Tests," in *Proceedings in Marine Science 9*. Editors T. Kusuda, Y. Hiroyuki, J. Spearman, and J. Z. Gailani (Amsterdam: Elsevier), 137–153. doi:10.1016/s1568-2692(08)80013-7

Hirayama, J., and Nakajima, T. (1977). Analytical Study of Turbidites, Otadai Formation, Boso Peninsula, Japan. *Sedimentology* 24, 747–779. doi:10.1111/j.1365-3091.1977.tb01914.x

Hodgetts, D., Drinkwater, N. J., Hodgson, J., Kavanagh, J., Flint, S. S., Keogh, K. J., et al. (2004). "Three-dimensional Geological Models from Outcrop Data Using Digital Data Collection Techniques: an Example from the Tanqua Karoo Depocentre, South Africa," in *Geological Prior Information: Informing Science and Engineering*. Editors A. C. Curtis and R. Wood (LondonLondon: Geological Society Special Publication), 57–75. doi:10.1144/gsl.sp.2004.239.01.05

Hodgson, D. M. (2009). Distribution and Origin of Hybrid Beds in Sand-Rich Submarine Fans of the Tanqua Depocentre, Karoo Basin, South Africa. *Mar. Pet. Geology* 26, 1940–1956. doi:10.1016/j.marpetgeo.2009.02.011

Hodgson, D. M., Flint, S. S., Hodgetts, D., Drinkwater, N. J., Johannessen, E. P., and Luthi, S. M. (2006). Stratigraphic Evolution of fine-grained Submarine Fan Systems, Tanqua Depocenter, Karoo Basin, South Africa. *J. Sediment. Res.* 76, 20–40. doi:10.2110/jsr.2006.03

Hodgson, D. M., Kane, I. A., Flint, S. S., Brunt, R. L., and Ortiz-Karpf, A. (2016). Time-transgressive Confinement on the Slope and the Progradation of basin-floor Fans: Implications for the Sequence Stratigraphy of Deep-Water Deposits. *J. Sediment. Res.* 86 (1), 73–86. doi:10.2110/jsr.2016.3

Hofstra, M., Hodgson, D. M., Peakall, J., and Flint, S. S. (2015). Giant Scour-Fills in Ancient Channel-Lobe Transition Zones: Formative Processes and Depositional Architecture. *Sediment. Geology* 329, 98–114. doi:10.1016/j.sedgeo.2015.09.004

Hofstra, M., Pontén, A. S. M., Peakall, J., Flint, S. S., Nair, K. N., and Hodgson, D. M. (2017). The Impact of fine-scale Reservoir Geometries on Streamline Flow Patterns in Submarine Lobe Deposits Using Outcrop Analogues from the Karoo Basin. *Pet. Geosci.* 23, 159–176. doi:10.1144/petgeo2016-087

Howlett, D. M., Gawthorpe, R. L., Ge, Z., Rotevatn, A., and Jackson, C. A. L. (2020). Turbidites, Topography and Tectonics: Evolution of Submarine Channel-lobe Systems in the Salt-influenced Kwanza Basin, Offshore Angola. *Basin Res.*

Imhansoloeva, T. M., Akintoye, A. E., Mayowa, I. P., Abdulkarim, R., Oguwuike, I. D., Olubukola, S., et al. (2011). Numerical Assessment and Analysis of Textural Deposits of beach Sediment: A Case Study of Ajah (Okun Mopo) Beach Lagos South West Nigeria. *Nat. Sci.* 9, 165–174.

Jegou, I., Savoye, B., Pirmez, C., and Droz, L. (2008). Channel-mouth Lobe Complex of the Recent Amazon Fan: the Missing Piece. *Mar. Geology.* 252, 62–77. doi:10.1016/j.margeo.2008.03.004

Jobe, Z. R., Sylvester, Z., Howes, N., Pirmez, C., Parker, A., Cantelli, A., et al. (2017). High-resolution, Millennial-Scale Patterns of Bed Compensation on a Sand-Rich Intraslope Submarine Fan, Western Niger Delta Slope. *Geol. Soc. America Bull.* 129, 23–37. doi:10.1130/b31440.1

Jobe, Z. R., Sylvester, Z., Pirmez, C., Prather, B., El-Gawad, S. A., Minisini, D., et al. (2014). Ultra-high Resolution Modern Analog Dataset from the Western Niger Delta Slope: Facies Architecture and Application to Turbidite Reservoirs. *Gulf Coast Assoc. Geol. Societies Trans.* 64, 543–546.

Johann, P., de Castro, D. D., and Barroso, A. S. (2001). Reservoir Geophysics: Seismic Pattern Recognition Applied to Ultra-deepwater Oilfield in Campos basin, Offshore Brazil. In SPE Latin American and Caribbean Petroleum Engineering Conference, Buenos Aires, Argentina (Richardson, TX: Society of Petroleum Engineers SPE), 69483. doi:10.2118/69483-MS

Johnson, S. D., Flint, S., Hinds, D., and De Ville Wickens, H. (2001). Anatomy, Geometry and Sequence Stratigraphy of basin Floor to Slope Turbidite Systems,

Tanqua Karoo, South Africa. *Sedimentology* 48, 987–1023. doi:10.1046/j.1365-3091.2001.00405.x

Jones, D. W., Large, S., McQueen, A., and Helmi, A. (2015). Reservoir Geology of the Paleocene Forties Sandstone Member in the Fram Discovery, UK Central North Sea. *Geol. Soc. Lond. Spec. Publications* 403, 219–246. doi:10.1144/sp403.13

Kane, I. A., Pontén, A. S. M., Vangdal, B., Eggenhuisen, J. T., Hodgson, D. M., and Spychala, Y. T. (2017). The Stratigraphic Record and Processes of Turbidity Current Transformation across Deep-marine Lobes. *Sedimentology* 64, 1236–1273. doi:10.1111/sed.12346

Ketzer, J. M., Carpentier, B., Le Gallo, Y., and Le Thiez, P. (2005). Geological Sequestration of CO2in Mature Hydrocarbon Fields. Basin and Reservoir Numerical Modelling of the Forties Field, North Sea. *Oil Gas Sci. Tech. Rev. IFP* 60, 259–273. doi:10.2516/ogst:2005016

Kidd, G. D. (1999). Fundamentals of 3-D Seismic Volume Visualization. *The Leading Edge* 18, 702–709. doi:10.1190/1.1438362

Kneller, B., and Buckee, C. (2000). The Structure and Fluid Mechanics of Turbidity Currents: A Review of Some Recent Studies and Their Geological Implications. *Sedimentology* 47, 62–94.

Lowry, P., Jenkins, C. D., and Phelps, D. J. (1993). January. Reservoir Scale Sandbody Architecture of Pliocene Turbidite Sequences, Long Beach Unit, Wilmington Oil Field, California. In SPE Annual Technical Conference and Exhibition, Houston, TX (Richardson, TX: Society of Petroleum Engineers), 26440. doi:10.2118/26440-ms

MacDonald, H. A., Peakall, J., Wignall, P. B., and Best, J. (2011). Sedimentation in Deep-Sea Lobe-Elements: Implications for the Origin of Thickening-Upward Sequences. *J. Geol. Soc.* 168, 319–332. doi:10.1144/0016-76492010-036]

Maier, K. L., Fildani, A., McHargue, T. R., Paull, C. K., Graham, S. A., and Caress, D. W. (2012). Punctuated Deep-Water Channel Migration: High-Resolution Subsurface Data from the Lucia Chica Channel System, Offshore California, U.S.A. *J. Sediment. Res.* 82, 1–8. doi:10.2110/jsr.2012.10

Maier, K. L., Fildani, A., Paull, C. K., Graham, S. A., McHargue, T. R., Caress, D. W., et al. (2011). The Elusive Character of Discontinuous Deep-Water Channels: New Insights from Lucia Chica Channel System, Offshore California. *Geology* 39, 327–330. doi:10.1130/g31589.1

Maier, K. L., Fildani, A., Paull, C. K., McHargue, T. R., Graham, S. A., and Caress, D. W. (2013). Deep-sea Channel Evolution and Stratigraphic Architecture from Inception to Abandonment from High-Resolution Autonomous Underwater Vehicle Surveys Offshore central California. *Sedimentology* 60, 935–960. doi:10.1111/j.1365-3091.2012.01371.x

Maier, K. L., Paull, C. K., Caress, D. W., Anderson, K., Nieminski, N. M., Lundsten, E., et al. (2020). Submarine-fan Development Revealed by Integrated High-Resolution Datasets from La Jolla Fan, Offshore California, U.S.A. *J. Sediment. Res.* 90 (5), 468–479. doi:10.2110/jsr.2020.22

Maier, K. L., Roland, E. C., Walton, M. A. L., Conrad, J. E., Brothers, D. S., Dartnell, P., et al. (2018). The Tectonically Controlled San Gabriel Channel-Lobe Transition Zone, Catalina Basin, Southern California Borderland. *J. Sediment. Res.* 88, 942–959. doi:10.2110/jsr.2018.50

Martinsen, O. J., Lien, T., Walker, R. G., and Lien, T. (2000). "Upper Carboniferous Deep Water Sediments, Western Ireland: Analogues for Passive Margin Turbidite Plays," in *Deep-Water Reservoirs of the World. Gulf Coast Section SEPM 20th Bob F. Perkins Research Conference*. Editors P. Weimer, R. M. Slatt, J. Coleman, N. C. Rosen, H. Nelson, A. H. Bouma, et al. 533–555. doi:10.5724/gcs.00.15.0533

Masalimova, L. U., Lowe, D. R., Sharman, G. R., King, P. R., and Arnot, M. J. (2016). Outcrop Characterization of a Submarine Channel-Lobe Complex: the Lower Mount Messenger Formation, Taranaki Basin, New Zealand. *Mar. Pet. Geology.* 71, 360–390. doi:10.1016/j.marpetgeo.2016.01.004

McHargue, T., Pyrcz, M. J., Sullivan, M. D., Clark, J. D., Fildani, A., Romans, B. W., et al. (2011). Architecture of Turbidite Channel Systems on the continental Slope: Patterns and Predictions. *Mar. Pet. Geology.* 28, 728–743. doi:10.1016/j.marpetgeo.2010.07.008

Métivier, F., Lajeunesse, E., and Cacas, M.-C. (2005). Submarine Canyons in the Bathtub. *J. Sediment. Res.* 75, 6–11. doi:10.2110/jsr.2005.002

Migeon, S., Ducassou, E., Le Gonidec, Y., Rouillard, P., Mascle, J., and Revel-Rolland, M. (2010). Lobe Construction and Sand/mud Segregation by Turbidity Currents and Debris Flows on the Western Nile Deep-Sea Fan (Eastern Mediterranean). *Sediment. Geology.* 229, 124–143. doi:10.1016/j.sedgeo.2010.02.011

Mulder, T., and Etienne, S. (2010). Lobes in Deep-Sea Turbidite Systems: State of the Art. *Sediment. Geology.* 229, 75–80. doi:10.1016/j.sedgeo.2010.06.011

Mutti, E. (1977). Distinctive Thin-Bedded Turbidite Facies and Related Depositional Environments in the Eocene Hecho Group (South-central Pyrenees, Spain). *Sedimentology* 24, 107–131. doi:10.1111/j.1365-3091.1977.tb00122.x

Mutti, E., and Ghibaudo, G. (1972). Un esempio di torbiditi di conoide sottomarina esterna: le Arenarie di San Salvatore (Formazione di Bobbio, Miocene) nell'Appennino di Piacenza. Torino, Italy: Accademia delle scienze, 40.

Mutti, E., and Normark, W. R. (1987). "Comparing Examples of Modern and Ancient Turbidite Systems: Problems and Concepts," in *Marine Clastic Sedimentology* (Dordrecht: Springer), 1–38. doi:10.1007/978-94-009-3241-8_1

Mutti, E., and Ricci Lucchi, F. (1972). Le torbiditi delt Apennino settentrionale: introduzione all'analisi di facies. *Memorie Società. Geologica Italiana* 11, 161–199.

Mutti, E., and Sonnino, M. (1981).*Compensation Cycles: A Diagnostic Feature of Turbidite sandstone Lobes*. Bologna, Italy: International Association of Sedimentologists, 2nd European Regional Meeting, 120–123.

Normark, W. R. (1978). Fan Valleys, Channels and Depositional Lobes on Modern Submarine Fans: Characteristics for Recognition of sandy Turbidite Environments. *Am. Assoc. Pet. Geologists Bull.* 62, 912–931.

Normark, W. R. (1970). Growth Patterns of Deep Sea Fans. *Am. Assoc. Pet. Geologists Bull.* 54, 2170–2195.

O'Connell, S., Ryan, W. B., and Normark, W. R. (1991). "Evolution of a Fan Channel on the Surface of the Outer Mississippi Fan: Evidence from Side-Looking Sonar," in *Seismic Facies and Sedimentary Processes of Submarine Fans and Turbidite Systems*. Editors P. Weimer and M. H. Link (New York: Springer), 365–381.

Oluboyo, A. P., Gawthorpe, R. L., Bakke, K., and Hadler-Jacobsen, F. (2014). Salt Tectonic Controls on Deep-Water Turbidite Depositional Systems: Miocene, Southwestern Lower Congo Basin, Offshore Angola. *Basin Res.* 26, 597–620. doi:10.1111/bre.12051

Paumard, V., Bourget, J., Payenberg, T., George, A. D., Ainsworth, R. B., Lang, S., et al. (2020). Controls on Deep-Water Sand Delivery beyond the Shelf Edge: Accommodation, Sediment Supply, and Deltaic Process Regime. *J. Sediment. Res.* 90 (1), 104–130. doi:10.2110/jsr.2020.2

Peakall, J., McCaffrey, B., and Kneller, B. (2000). A Process Model for the Evolution, Morphology, and Architecture of Sinuous Submarine Channels. *J. Sediment. Res.* 70 (3), 434–448.

Picot, M., Droz, L., Marsset, T., Dennielou, B., and Bez, M. (2016). Controls on Turbidite Sedimentation: Insights from a Quantitative Approach of Submarine Channel and Lobe Architecture (Late Quaternary Congo Fan). *Mar. Pet. Geology.* 72, 423–446. doi:10.1016/j.marpetgeo.2016.02.004

Pierce, C. S., Haughton, P. D. W., Shannon, P. M., Pulham, A. J., Barker, S. P., and Martinsen, O. J. (2018). Variable Character and Diverse Origin of Hybrid Event Beds in a sandy Submarine Fan System, Pennsylvanian Ross Sandstone Formation, Western Ireland. *Sedimentology* 65, 952–992. doi:10.1111/sed.12412

Pirmez, C., Beaubouef, R. T., Friedmann, S. J., and Mohrig, D. C. (2000). "Equilibrium Profile and Baselevel in Submarine Channels: Examples from Late Pleistocene Systems and Implications for the Architecture of Deepwater Reservoirs," in *Deep-water Reservoir of the World*. Editors P. Weimer, R. M. Slatt, A. H. Bouma, and D. T. Lawrence Gulf Coast Section SEPM Foundation 20th Annual Research Conference, Houston, TX, 782–805. doi:10.5724/gcs.00.15.0782

Posamentier, H. W., and Kolla, V. (2003). Seismic Geomorphology and Stratigraphy of Depositional Elements in Deep-Water Settings. *J. Sediment. Res.* 73, 367–388. doi:10.1306/111302730367

Posamentier, H. W., Wisman, P. S., and Plawman, T. (2000). "Deep Water Depositional Systems-Ultra-Deep Makassar Strait, Indonesia," in *Deep-Water Reservoirs of the World: Gulf Coast Society of the Society of Economic Paleontologists and Mineralogists Foundation, 20th Annual Research*

Conference. Editors P. Weimer, R. M. Slatt, J. Coleman, N. C. Rosen, H. Nelson, A. H. Bouma, et al. 806–816. doi:10.5724/gcs.00.15.0806

Prather, B. E., Booth, J. R., Steffens, G. S., and Craig, P. A. (1998). Classification, Lithologic Calibration and Stratigraphic Succession of Seismic Facies from Intraslope Basins, Deep Water Gulf of Mexico. *U.S.A. Am. Assoc. Pet. Geologists Bull.* 82, 701–728.

Prather, B. E. (2000). Calibration and Visualization of Depositional Process Models for Above-Grade Slopes: a Case Study from the Gulf of Mexico. *Mar. Pet. Geology.* 17, 619–638. doi:10.1016/s0264-8172(00)00015-5

Prather, B. E. (2003). Controls on Reservoir Distribution, Architecture and Stratigraphic Trapping in Slope Settings. *Mar. Pet. Geology.* 20, 529–545. doi:10.1016/j.marpetgeo.2003.03.009

Prather, B. E., Pirmez, C., Sylvester, Z., and Prather, D. S. (2012a). "Stratigraphic Response to Evolving Geomorphology in a Submarine Apron Perched on the Upper Niger Delta Slope," in *Application of the Principles of Seismic Geomorphology to continental Slope and Base-Of-Slope Systems: Case Studies from Seafloor and Near-Seafloor Analogues*. Editors B. E. Prather, M. E. Deptuck, D. Mohrig, B. Van Hoorn, and R. B. Wynn (Tulsa, OK: SEPM Special Publication), 145–161. doi:10.2110/pec.12.99.0145

Prather, B. E., Pirmez, C., Winker, C. D., Deptuck, M. E., and Mohrig, D. (2012b). Stratigraphy of Linked Intraslope Basins: Brazos-Trinity System Western Gulf of Mexico. *SEPM, Spec. Publ.* 99, 83–109. doi:10.2110/pec.12.99.0083

Prélat, A., Covault, J. A., Hodgson, D. M., Fildani, A., and Flint, S. S. (2010). Intrinsic Controls on the Range of Volumes, Morphologies, and Dimensions of Submarine Lobes. *Sediment. Geology.* 232, 66–76. doi:10.1016/j.sedgeo.2010.09.010

Prélat, A., Hodgson, D. M., and Flint, S. S. (2009). Evolution, Architecture and Hierarchy of Distributary Deep-water Deposits: a High-resolution Outcrop Investigation from the Permian Karoo Basin, South Africa. *Sedimentology* 56, 2132–2154. doi:10.1111/j.1365-3091.2009.01073.x

Prélat, A., and Hodgson, D. M. (2013). The Full Range of Turbidite Bed Thickness Patterns in Submarine Lobes: Controls and Implications. *J. Geol. Soc.* 170, 209–214. doi:10.1144/jgs2012-056

P. Weimer, R. M. Slatt, J. Coleman, N. C. Rossen, H. Nelson, A. H. Bouma, et al. (2000). "Deep-water Reservoirs of the World," in Gulf Coast Section SEPM Foundation 20th Annual Research Conference, Houston, TX.

Pyles, D. R., and Jennette, D. C. (2009). Geometry and Architectural Associations of Co-genetic Debrite-Turbidite Beds in basin-margin Strata, Carboniferous Ross Sandstone (Ireland): Applications to Reservoirs Located on the Margins of Structurally Confined Submarine Fans. *Mar. Pet. Geology.* 26, 1974–1996. doi:10.1016/j.marpetgeo.2009.02.018

Pyles, D. R., Strachan, L. J., and Jennette, D. C. (2014). Lateral Juxtapositions of Channel and Lobe Elements in Distributive Submarine Fans: Three-Dimensional Outcrop Study of the Ross Sandstone and Geometric Model. *Geosphere* 10, 1104–1122. doi:10.1130/ges01042.1

Reading, H. G., and Richards, M. (1994). Turbidite Systems in Deep-Water basin Margins Classified by Grain Size and Feeder System. *Am. Assoc. Pet. Geologists Bull.* 78, 792–822.

Remacha, E., Fernandez, L. P., and Maestro, E. (2005). The Transition between Sheet-like Lobe and basin-plain Turbidites in the Hecho Basin (South-Central Pyrenees, Spain). *J. Sediment. Res.* 75, 798–819. doi:10.2110/jsr.2005.064

Rowland, J. C., Hilley, G. E., and Fildani, A. (2010). A Test of Initiation of Submarine Leveed Channels by Deposition Alone. *J. Sediment. Res.* 80, 710–727. doi:10.2110/jsr.2010.067

Ruzuar, A. P., Schneinder, R., Saller, A. H., and Noah, J. T., 2005. Linked Lowstand Delta to Basin-Floor Fan Deposition, Offshore East Kalimantan: An Analogue for Deep-Water Reservoir Systems. Proceedings, Indonesian Petroleum Association Thirtieth Annual Convention and Exhibition, 2005. 467–481.

Saller, A., Dharmasamadhi, I. N. W., Lilburn, T., and Ryan, E. (2010). "Seismic Geomorphology of Submarine Slopes: Channel-Levee Complexes versus Slope Valleys and Canyons, Pleistocene, East Kalimantan, Indonesia," in *Seismic Imaging of Depositional and Geomorphic Systems. Gulf Coast Section SEPM, 30th Annual Conference*. Editors L. J. Wood, T. T. Simo, and N. C. Rosen, 433–471. doi:10.5724/gcs.10.30.0433

Saller, A. H., Noah, J. T., Ruzuar, A. P., and Schneider, R. (2004). Linked Lowstand delta to basin-floor Fan Deposition, Offshore Indonesia: An Analog for Deep-Water Reservoir Systems. *Bulletin* 88, 21–46. doi:10.1306/09030303003

Saller, A. H., Noah, J. T., Schneider, R., and Ruzuar, A. P., 2003, Lowstand Deltas and a Basin-Floor Fan, Pleistocene, Offshore East Kalimantan, Indonesia. In: Margin deltas and linked down slope petroleum systems: Global significance and future exploration potential. Gulf Coast Section SEPM Foundation 23rd Annual Bob F. Perkins Research Conference. 421–439. doi:10.5724/gcs.03.23.0421

Saller, A., Werner, K., Sugiaman, F., Cebastiant, A., May, R., Glenn, D., et al. (2008). Characteristics of Pleistocene Deep-Water Fan Lobes and Their Application to an Upper Miocene Reservoir Model, Offshore East Kalimantan, Indonesia. *Bulletin* 92, 919–949. doi:10.1306/03310807110

Shanmugam, G., Shrivastava, S. K., and Das, B. (2009). Sandy Debrites and Tidalites of Pliocene Reservoir Sands in Upper-Slope Canyon Environments, Offshore Krishna-Godavari Basin (India): Implications. *J. Sediment. Res.* 79, 736–756. doi:10.2110/jsr.2009.076

So, Y. S., Rhee, C. W., Choi, P.-Y., Kee, W.-S., Seo, J. Y., and Lee, E.-J. (2013). Distal Turbidite Fan/lobe Succession of the Late Paleozoic Taean Formation, Western Korea. *Geosci. J.* 17, 9–25. doi:10.1007/s12303-013-0016-0

Spychala, Y. T., Hodgson, D. M., Flint, S. S., and Mountney, N. P. (2015). Constraining the Sedimentology and Stratigraphy of Submarine Intraslope Lobe Deposits Using Exhumed Examples from the Karoo Basin, South Africa. *Sediment. Geology.* 322, 67–81. doi:10.1016/j.sedgeo.2015.03.013

Steffens, G. S., Biegert, E. K., Scott Sumner, H., and Bird, D. (2003). Quantitative Bathymetric Analyses of Selected deepwater Siliciclastic Margins: Receiving basin Configurations for deepwater Fan Systems. *Mar. Pet. Geology.* 20, 547–561. doi:10.1016/j.marpetgeo.2003.03.007

Stow, D. A. V. (1986). "Deep Clastic Seas," in *Sedimentary Environments and Facies*. Editor H. G. Reading (Oxford: Blackwell Scientific Publications), 399–444.

Stow, D. A. V. (1985). "Deep-sea Clastics: where Are We and where Are We Going?," in *Sedimentology: Recent Developments and Applied Aspects*. Editors P. J. Brenchley and B. P. J. Williams (London: Geological Society [London] Special Publication), 67–93. doi:10.1144/gsl.sp.1985.018.01.05

Straub, K. M., and Pyles, D. R. (2012). Quantifying the Hierarchical Organization of Compensation in Submarine Fans Using Surface Statistics. *J. Sediment. Res.* 82 (11), 889–898. doi:10.2110/jsr.2012.73

Sullivan, M., Jensen, G., Goulding, F., Jennette, D., Foreman, L., and Stern, D. (2000). "Architectural Analysis of Deep-Water Outcrops: Implications for Exploration and Development of the Diana Sub-Basin, Western Gulf of Mexico," in *Deep-Water Reservoirs of the World. Gulf Coast Section SEPM 20th Bob F. Perkins Research Conference*. Editors P. Weimer, R. M. Slatt, J. Coleman, N. C. Rosen, H. Nelson, A. H. Bouma, et al. 1010–1031. doi:10.5724/gcs.00.15.1010

Sylvester, Z., Deptuck, M. E., Prather, B. E., Pirmez, C., and O'Byrne, C. (2012). "Seismic Stratigraphy of a Shelf-Edge delta and Linked Submarine Channels in the Northeastern Gulf of Mexico," in *Application of the Principles of Seismic Geomorphology to continental Slope and Base-Of-Slope Systems: Case Studies from Seafloor and Near-Seafloor Analogues*. Editors B. E. Prather, M. E. Deptuck, D. Mohrig, B. Van Hoorn, and R. B. Wynn (Tulsa, OK: SEPM Special Publication), 31–59. doi:10.2110/pec.12.99.0031

Terlaky, V., Rocheleau, J., and Arnott, R. W. C. (2016). Stratal Composition and Stratigraphic Organization of Stratal Elements in an Ancient Deep-marine basin-floor Succession, Neoproterozoic Windermere Supergroup, British Columbia, Canada. *Sedimentology* 63, 136–175. doi:10.1111/sed.12222

Twichell, D. C., Schwab, W. C., Nelson, C. H., Kenyon, N. H., and Lee, H. J. (1992). Characteristics of a sandy Depositional Lobe on the Outer Mississippi Fan from SeaMARC IA Sidescan Sonar Images. *Geol.* 20, 689–692. doi:10.1130/0091-7613(1992)020<0689:coasdl>2.3.co;2

Twichell, D., Nelson, C. H., Kenyon, N., and Schwab, W. (2009). "The Influence of External Processes on the Holocene Evolution of the Mississippi Fan," in *External Controls on Deepwater Depositional Systems*. Editors B. Kneller, O. J. Martinsen, and W. D. McCaffrey (Tulsa, OK: SEPM Special Publication), 145–157. doi:10.2110/sepmsp.092.145

Van der Merwe, W. C., Hodgson, D. M., Brunt, R. L., and Flint, S. S. (2014). Depositional Architecture of Sand-Attached and Sand-Detached Channel-Lobe Transition Zones on an Exhumed Stepped Slope Mapped over a 2500 Km2 Area. *Geosphere* 10, 1076–1093. doi:10.1130/GES0103510.1130/ges01035.1

Walker, R. G. (1978). Deep-water sandstone Facies and Ancient Submarine Fans: Models for Exploration for Stratigraphic Traps. *Am. Assoc. Pet. Geologists Bull.* 62, 932–966.

Yang, S.-Y., and Kim, J. W. (2014). Pliocene basin-floor Fan Sedimentation in the Bay of Bengal (Offshore Northwest Myanmar). *Mar. Pet. Geology.* 49, 45–58. doi:10.1016/j.marpetgeo.2013.09.007

Conflict of Interest: The authors declare that the research was conducted in the absence of any commercial or financial relationships that could be construed as a potential conflict of interest.

Publisher's Note: All claims expressed in this article are solely those of the authors and do not necessarily represent those of their affiliated organizations, or those of the publisher, the editors and the reviewers. Any product that may be evaluated in this article, or claim that may be made by its manufacturer, is not guaranteed or endorsed by the publisher.